

Time dependence in $B \rightarrow V\ell\ell$ decays

Sébastien Descotes-Genon^a and Javier Virto^b

^a *Laboratoire de Physique Théorique, CNRS/Univ. Paris-Sud (UMR 8627)
91405 Orsay Cedex, France*

^b *Theoretische Physik 1, Naturwissenschaftlich-Technische Fakultät,
Universität Siegen, 57068 Siegen, Germany*

Abstract

We discuss the theory and phenomenology of $B_{d,s} \rightarrow V(\rightarrow M_1 M_2)\ell\ell$ decays in the presence of neutral-meson mixing. We derive expressions for the time-dependent angular distributions for decays into CP eigenstates, and identify the relevant observables that can be extracted from time-integrated and time-dependent analyses with or without tagging, with a focus on the difference between measurements at B -factories and hadronic machines. We construct two observables of interest, which we call Q_8^- and Q_9 , and which are theoretically clean at large recoil. We compute these two observables in the Standard Model, and show that they have good potential for New Physics searches by considering their sensitivity to benchmark New Physics scenarios consistent with current $b \rightarrow s\ell\ell$ data. These results apply to decays such as $B_d \rightarrow K^*(\rightarrow K_S\pi^0)\ell\ell$, $B_s \rightarrow \phi(\rightarrow K_S K_L)\ell\ell$ and $B_s \rightarrow \phi(\rightarrow K^+ K^-)\ell\ell$.

1 Introduction

Rare B decays mediated by flavour-changing neutral currents constitute a unique playground to test the Standard Model (SM) and search for New Physics (NP). Among these, processes mediated by the quark-level $b \rightarrow s\ell\ell$ transition have received a great deal of attention following a large programme of measurements at B -factories, LHCb and CMS: branching ratios, CP asymmetries and angular distributions of $B \rightarrow K^{(*)}\mu^+\mu^-$ [1–11] and $B_s \rightarrow \phi\mu^+\mu^-$ [12] decays, the branching ratio $\mathcal{B}(B_s \rightarrow \mu^+\mu^-)$ [13–15], and inclusive $B \rightarrow X_s\ell\ell$ observables [16, 17]. Global fits to all $b \rightarrow s\gamma$ and $b \rightarrow s\ell\ell$ data have recently uncovered a pattern of tensions between theory and experiment, triggered by the analysis of the $B \rightarrow K^*\mu^+\mu^-$ angular distribution [18–21], and followed by the measurement of the ratio $R_K \equiv \mathcal{B}(B \rightarrow K\mu\mu)/\mathcal{B}(B \rightarrow Kee)$, which is consistent with New Physics in

$B \rightarrow K^* \mu \mu$ data and hints at lepton-flavour non-universality [22–28]. In this context, the study of new independent $b \rightarrow s \ell \ell$ observables is of great interest, as a means to gather evidence for (or against) these tensions, and to fingerprint the resulting New Physics.

When dealing with decays of *neutral* B mesons, experimental observables are affected by particle-antiparticle mixing (oscillations), with the decaying meson being either a B or a \bar{B} depending on the time of decay. In the case of flavour-non-specific decays –such as decays into CP eigenstates– in which the final state can arise from the decay of both B and \bar{B} mesons, the mixing and decay processes interfere quantum-mechanically, leading to interesting phenomenological consequences (for a review see for instance Refs. [29,34]). In particular, new observables arise compared to the case without mixing. These observables depend on the experimental set-up (B -factory or hadronic machine), the presence of flavour tagging of the decaying B -meson, and the possibility to perform time-dependent measurements (in contrast to the limitation to time-integrated observables). In the case of $b \rightarrow s \ell \ell$ transitions, these effects have been so far taken into account in the untagged time-integrated measurements of $B_s \rightarrow \phi \mu^+ \mu^-$ [30] and $B_s \rightarrow \mu^+ \mu^-$ [31] at the LHC, (see also the discussion in Ref. [32] in the case of $B_s \rightarrow VV$ decays). Time-dependent angular analyses of $B_{d,s} \rightarrow V \ell \ell$ with tagging are much more challenging experimentally, but might be reached at a high-luminosity flavour factory such as Belle-II [33].

In this paper we develop the theoretical framework and study the phenomenological advantages of time-dependent $B_{d,s} \rightarrow V \ell \ell$ decays, spelling out the new observables that can be accessed, as well as the opportunities for New Physics searches, both at B -factories and hadronic machines. While the formalism is valid for any decay of the type $B_{d,s} \rightarrow V(\rightarrow M_1 M_2) \ell \ell$ with $M_1 M_2$ a CP eigenstate, we identify the following modes of interest:

- $B_d \rightarrow K^{*0}(\rightarrow K_S \pi^0) \ell^+ \ell^-$
- $B_s \rightarrow \phi(\rightarrow K_S K_L) \ell^+ \ell^-$
- $B_s \rightarrow \phi(\rightarrow K^+ K^-) \ell^+ \ell^-$

As a summary of the main points to be discussed below, we shall see that:

- In the presence of mixing, the time-dependent angular distributions exhibit a new type of angular coefficients, h_i and s_i , apart from the usual coefficients accessible from flavour-specific decays, J_i and \bar{J}_i , c.f. Eqs. (25),(26).
- Time-integrated CP-averaged rates and CP-asymmetries, as measured at hadronic machines, are affected by mixing effects in two ways, c.f. Eqs. (42),(43): 1) The terms with $J_i \pm \bar{J}_i$ are multiplied by the factors $1/(1-y^2)$ and $1/(1+x^2)$ respectively, with $y = \Delta\Gamma/(2\Gamma)$ and $x = \Delta m/\Gamma$. 2) New contributions proportional to the coefficients h_i and s_i arise. At B -factories only the first type of corrections appear, and time-integrated quantities are independent of the coefficients s_i and h_i , c.f. Eqs.(44),(45).

- We identify s_8 and s_9 as new observables of interest, which can be extracted most conveniently from a time-dependent analysis with flavour tagging. Theoretically clean observables can be built from s_8 and s_9 ; two such observables are Q_8^- and Q_9 , which are clean at large hadronic recoil. These observables contain independent information, not accessible from flavour-specific decays. Such observables could be studied, for instance, at a high-luminosity flavour factory, where a separation between B and \bar{B} samples would be possible together with a study of time dependence of the decay process.
- The observables Q_8^- and Q_9 can be predicted in the Standard Model with small uncertainties (see Fig. 1). In particular, Q_9 measures right-handed currents: in the case of a $b \rightarrow s$ transition, $Q_9^{\text{SM}} \simeq -\cos(\phi_q - 2\beta_s)$ to a very good precision, with ϕ_q the mixing angle of the B_q system. In addition, these observables are very sensitive to New Physics scenarios consistent with current $b \rightarrow s\gamma$ and $b \rightarrow s\ell\ell$ data, such as models with Z' bosons with vector and/or axial couplings to fermions.

The structure of this article is the following. We begin in Section 2 with a discussion on time-dependent angular distributions: In Section 2.1 we review the basic facts of $B \rightarrow V\ell\ell$ decays without mixing. In Section 2.2 we address the CP parities associated to transversity amplitudes for $B \rightarrow V\ell\ell$ decays into CP eigenstates. In Section 2.3 we derive the expressions for the time-dependent angular distributions, and identify the new angular observables $h_i(s)$ and $s_i(s)$ that arise in the presence of mixing, demonstrating in Section 2.4 that $s_{5,6s,8,9}(s)$ contain independent information not accessible from the angular distribution of flavour-specific decays. In Section 3 we discuss in detail the two types of observables that can be obtained from the distributions in the presence of mixing: time-integrated (Section 3.1) and time-dependent (Section 3.2) observables. We also define the observables Q_8^- and Q_9 , which are form-factor-independent at large recoil, and we provide simplified expressions at the leading order of the effective theory in this limit. Standard Model predictions for these observables and New Physics opportunities are discussed in Section 4. Finally, we conclude in Section 5. Some details are relegated to the appendices. In Appendix A we discuss the kinematics of CP-conjugated $B \rightarrow V(\rightarrow M_1 M_2)\ell\ell$ decays in terms of momentum invariants and the different conventions for the kinematic angles that appear in the angular distributions. In Appendix B we recall the determination of the CP parity for the different transversity amplitudes. In Appendix C we collect the expressions for the coefficients $h_i(s)$ and $s_i(s)$ in terms of transversity amplitudes.

2 Time-dependent angular distributions

2.1 $B \rightarrow V\ell\ell$ decays without mixing

We first recall a few elements of the analysis of the exclusive $b \rightarrow s\ell\ell$ decays of the type $B \rightarrow V(\rightarrow M_1 M_2)\ell\ell$. In this subsection, we consider a situation where no mixing occurs, and where the $M_1 M_2$ state is not (necessarily) a CP-eigenstate.

This process is described by the usual effective Hamiltonian, with SM operators plus (potentially) NP operators with chirality flip, scalar or tensor structure [39, 42]:

$$\mathcal{H}_{\text{eff}} = \frac{4G_F}{\sqrt{2}} \left[\lambda_u \mathcal{C}_1 \mathcal{O}_1^u + \lambda_c \mathcal{C}_1 \mathcal{O}_1^c - \lambda_t \sum_{i \in I} \mathcal{C}_i \mathcal{O}_i \right], \quad (1)$$

where $\lambda_q = V_{qb}V_{qs}^*$ and $I = \{3, 4, 5, 6, 8, 7, 7', 9, 9', 10, 10', S, S', P, P', T, T'\}$. The operators $\mathcal{O}_{1,\dots,6}$ and \mathcal{O}_8 are hadronic operators of the type $(\bar{s}\Gamma b)(\bar{q}\Gamma' q)$ and $(\bar{s}\sigma^{\mu\nu}T_a P_R b)G_{\mu\nu}^a$ respectively [43], and contribute to $b \rightarrow s\ell\ell$ processes through a loop coupled to an electromagnetic current (via $b \rightarrow s\gamma^* \rightarrow s\ell\ell$). These operators are not likely to receive significant contributions from NP, as these would show up in non-leptonic B decay amplitudes¹. The operators $\mathcal{O}_{7^{(\prime)}, 9^{(\prime)}, 10^{(\prime)}, S^{(\prime)}, P^{(\prime)}, T^{(\prime)}}$ are given by:

$$\begin{aligned} \mathcal{O}_{7^{(\prime)}} &= \frac{e}{(4\pi)^2} m_b [\bar{s}\sigma^{\mu\nu} P_{R(L)} b] F_{\mu\nu}, & \mathcal{O}_{S^{(\prime)}} &= \frac{e^2}{(4\pi)^2} [\bar{s} P_{R(L)} b] [\bar{\ell}\ell], \\ \mathcal{O}_{9^{(\prime)}} &= \frac{e^2}{(4\pi)^2} [\bar{s}\gamma^\mu P_{L(R)} b] [\bar{\ell}\gamma_\mu \ell], & \mathcal{O}_{P^{(\prime)}} &= \frac{e^2}{(4\pi)^2} [\bar{s} P_{R(L)} b] [\bar{\ell}\gamma_5 \ell], \\ \mathcal{O}_{10^{(\prime)}} &= \frac{e^2}{(4\pi)^2} [\bar{s}\gamma^\mu P_{L(R)} b] [\bar{\ell}\gamma_\mu \gamma_5 \ell], & \mathcal{O}_{T^{(\prime)}} &= \frac{e^2}{(4\pi)^2} [\bar{s}\sigma_{\mu\nu} P_{R(L)} b] [\bar{\ell}\sigma^{\mu\nu} P_{R(L)} \ell], \end{aligned} \quad (2)$$

with $\sigma^{\mu\nu} = i[\gamma^\mu, \gamma^\nu]/2$ and $P_{L,R} = (1 \mp \gamma_5)/2$. In the SM, and at a scale $\mu_b = \mathcal{O}(m_b)$, the only non-negligible Wilson coefficients regarding the the operators in Eq. (2) are $\mathcal{C}_7^{\text{SM}}(\mu_b) \simeq -0.3$, $\mathcal{C}_9^{\text{SM}}(\mu_b) \simeq 4$ and $\mathcal{C}_{10}^{\text{SM}}(\mu_b) \simeq -4$ (see Table 2); but all might be affected by NP. Contributions to $B \rightarrow V\ell\ell$ from electromagnetic dipole operators $\mathcal{O}_{7^{(\prime)}}$ are (like hadronic contributions) of the type $b \rightarrow s\gamma^* \rightarrow s\ell\ell$. Contributions from semileptonic operators $\mathcal{O}_{9^{(\prime)}, 10^{(\prime)}, S^{(\prime)}, P^{(\prime)}, T^{(\prime)}}$ are factorizable and their matrix elements can be written as

$$\langle V\ell\ell | \mathcal{O}_{\text{sl}} | B \rangle = \langle V | \Gamma^M | B \rangle \langle \ell\ell | \Gamma'_M | 0 \rangle, \quad (3)$$

where M denotes a collection of Lorentz indices. It is clear that all hadronic, dipole, and semileptonic contributions can be recast as decays of the form

$$B \rightarrow V(\rightarrow M_1 M_2) N(\rightarrow \ell^+ \ell^-), \quad (4)$$

¹New Physics contributions at the $\sim 10\%$ level to the operators \mathcal{O}_1 , \mathcal{O}_2 is not excluded [64]. However, this should have a small impact on $b \rightarrow s\ell\ell$ where the effect of semileptonic operators dominates.

where N has the quantum numbers of a boson, whose coupling pattern is determined by the operators arising in the effective Hamiltonian. In the SM, the structure of $\mathcal{O}_7, \mathcal{O}_9, \mathcal{O}_{10}$ shows that N are spin-1 particles, coupling to both left- and right-handed fermions. This is in agreement with the presence of γ^* and Z penguin contributions, but it is also able to reproduce the contribution from box diagrams involving two W bosons and a neutrino ($((V-A)(V-A))$ structure in the SM). In an extension of the SM yielding scalar (tensor) operators, one should add N bosons with spin 0 (spin 2 respectively).

We will work under the following assumptions, inspired by the situation in the SM and in its most usual extensions

- CP might be violated in the decay $B \rightarrow VN$, but it is conserved in the decay $N \rightarrow \ell^+ \ell^-$.
- N can have spin 0 or spin 1, but not spin 2 (no tensor currents in the effective Hamiltonian).

It proves useful to analyse such decays in terms of transversity amplitudes. Let us call

$$M_{mn} = \epsilon_V^{*\mu}(m) \epsilon_N^{*\nu}(n) M_{\mu\nu} \quad (5)$$

the helicity amplitudes for this decay, where m and n denote the polarisations of the meson V and the virtual boson N decaying into the dilepton pair, respectively.

If N has spin 1, as the initial decaying particle has spin 0, the only combination of helicity amplitudes allowed are $(m, n) = (0, 0), (+1, +1), (-1, -1), (0, t)$, where t denotes the timelike polarisation. One can then define the transversity amplitudes [39, 45, 49]

$$A_\perp = \frac{M_{+1,+1} - M_{-1,-1}}{\sqrt{2}} \quad A_\parallel = \frac{M_{+1,+1} + M_{-1,-1}}{\sqrt{2}} \quad A_0 = M_{0,0} \quad A_t = M_{0,t} . \quad (6)$$

The spin-1 N particle couples to the lepton pair either through $\bar{\ell} \gamma_\mu P_L \ell$ or $\bar{\ell} \gamma_\mu P_R \ell$, and we can further separate left- from right-handed components in the amplitudes: $A_0^L, A_0^R, A_\parallel^L, A_\parallel^R, A_\perp^L, A_\perp^R$. On the other hand, due to current conservation and the structure of the time-like polarisation $\epsilon_N^{*\nu}(t) \propto (p_{\ell^+} + p_{\ell^-})^\nu$, one can see that A_t corresponds to a pure axial coupling to the lepton pair, vanishing in the massless limit. In the case where N is spin 0, the only combination of helicity amplitudes allowed is $(m, n) = (0, 0)$. The effect of a spin-0 particle with a pseudoscalar coupling to leptons can be absorbed into A_t , whereas a scalar coupling requires a new amplitude, called A_S .

The spin-summed differential decay distribution is given by [45, 65]

$$\begin{aligned} \frac{d^4 \Gamma(B \rightarrow V(\rightarrow M_1 M_2) \ell^+ \ell^-)}{ds d\cos \theta_M d\cos \theta_l d\phi} = & \frac{9}{32\pi} \left[J_{1s} \sin^2 \theta_M + J_{1c} \cos^2 \theta_M + J_{2s} \sin^2 \theta_M \cos 2\theta_l \right. \\ & + J_{2c} \cos^2 \theta_M \cos 2\theta_l + J_3 \sin^2 \theta_M \sin^2 \theta_l \cos 2\phi + J_4 \sin 2\theta_M \sin 2\theta_l \cos \phi \\ & + J_5 \sin 2\theta_M \sin \theta_l \cos \phi + J_{6s} \sin^2 \theta_M \cos \theta_l + J_{6c} \cos^2 \theta_M \cos \theta_l \\ & \left. + J_7 \sin 2\theta_M \sin \theta_l \sin \phi + J_8 \sin 2\theta_M \sin 2\theta_l \sin \phi + J_9 \sin^2 \theta_M \sin^2 \theta_l \sin 2\phi \right] , \end{aligned} \quad (7)$$

in terms of the invariant mass of the lepton pair s , and three kinematical angles $\theta_\ell, \theta_M, \phi$ (see Appendix A). The coefficients of the distribution $J_i(s)$ contain interferences of the form $\text{Re}[A_X A_Y^*]$ and $\text{Im}[A_X A_Y^*]$ between the eight transversity amplitudes:

$$A_0^L, A_0^R, A_\parallel^L, A_\parallel^R, A_\perp^L, A_\perp^R, A_t, A_S, \quad (8)$$

and are given by

$$\begin{aligned} J_{1s} &= \frac{(2 + \beta_\ell^2)}{4} [|A_\perp^L|^2 + |A_\parallel^L|^2 + |A_\perp^R|^2 + |A_\parallel^R|^2] + \frac{4m_\ell^2}{s} \text{Re}(A_\perp^L A_\perp^{R*} + A_\parallel^L A_\parallel^{R*}), \\ J_{1c} &= |A_0^L|^2 + |A_0^R|^2 + \frac{4m_\ell^2}{s} [|A_t|^2 + 2\text{Re}(A_0^L A_0^{R*})] + \beta_\ell^2 |A_S|^2, \\ J_{2s} &= \frac{\beta_\ell^2}{4} [|A_\perp^L|^2 + |A_\parallel^L|^2 + |A_\perp^R|^2 + |A_\parallel^R|^2], \quad J_{2c} = -\beta_\ell^2 [|A_0^L|^2 + |A_0^R|^2], \\ J_3 &= \frac{1}{2}\beta_\ell^2 [|A_\perp^L|^2 - |A_\parallel^L|^2 + |A_\perp^R|^2 - |A_\parallel^R|^2], \quad J_4 = \frac{1}{\sqrt{2}}\beta_\ell^2 [\text{Re}(A_0^L A_\parallel^{L*} + A_0^R A_\parallel^{R*})], \\ J_5 &= \sqrt{2}\beta_\ell \left[\text{Re}(A_0^L A_\perp^{L*} - A_0^R A_\perp^{R*}) - \frac{m_\ell}{\sqrt{s}} \text{Re}(A_\parallel^L A_S^* + A_\parallel^{R*} A_S) \right], \\ J_{6s} &= 2\beta_\ell [\text{Re}(A_\parallel^L A_\perp^{L*} - A_\parallel^R A_\perp^{R*})], \quad J_{6c} = 4\beta_\ell \frac{m_\ell}{\sqrt{s}} \text{Re}(A_0^L A_S^* + A_0^{R*} A_S), \\ J_7 &= \sqrt{2}\beta_\ell \left[\text{Im}(A_0^L A_\parallel^{L*} - A_0^R A_\parallel^{R*}) + \frac{m_\ell}{\sqrt{s}} \text{Im}(A_\perp^L A_S^* - A_\perp^{R*} A_S) \right], \\ J_8 &= \frac{1}{\sqrt{2}}\beta_\ell^2 [\text{Im}(A_0^L A_\perp^{L*} + A_0^R A_\perp^{R*})], \quad J_9 = \beta_\ell^2 [\text{Im}(A_\parallel^{L*} A_\perp^L + A_\parallel^{R*} A_\perp^R)], \end{aligned} \quad (9)$$

where $\beta_\ell = \sqrt{1 - 4m_\ell^2/s}$. Similar expressions hold for the CP-conjugate decay $\bar{B} \rightarrow \bar{V}(\rightarrow \bar{M}_1 \bar{M}_2)\ell^+ \ell^-$, with angular coefficients \bar{J}_i involving amplitudes denoted by \bar{A}_X , and obtained from the A_X by conjugating all weak phases². The form of the angular distribution for the CP-conjugated decay, however, depends on the way the kinematical variables are defined. In the case in which the *same* conventions are used irrespective of whether the decaying meson is a B or a \bar{B} , we have (see Appendix A):

$$\frac{d\Gamma[B \rightarrow V(\rightarrow M_1 M_2)\ell^+ \ell^-]}{ds \, d\cos\theta_\ell \, d\cos\theta_M \, d\phi} = \sum_i J_i(s) f_i(\theta_\ell, \theta_M, \phi) \quad (10)$$

$$\frac{d\Gamma[\bar{B} \rightarrow \bar{V}(\rightarrow \bar{M}_1 \bar{M}_2)\ell^+ \ell^-]}{ds \, d\cos\theta_\ell \, d\cos\theta_M \, d\phi} = \sum_i \zeta_i \bar{J}_i(s) f_i(\theta_\ell, \theta_M, \phi) \quad (11)$$

where $f_i(\theta_\ell, \theta_M, \phi)$ are defined by Eq. (7), and

$$\zeta_i = 1 \quad \text{for } i = 1s, 1c, 2s, 2c, 3, 4, 7; \quad \zeta_i = -1 \quad \text{for } i = 5, 6s, 6c, 8, 9. \quad (12)$$

²This is opposite to the notation used in ref. [39] for B and \bar{B} decays, but in agreement with general discussions on CP-violation.

We stress that this result arises just from the identification of kinematics of CP-conjugate decays, and does not rely on any intrinsic CP-parity of the initial or final states involved.

2.2 CP-parity of final states and decays into CP eigenstates

The separation into transversity amplitudes not only simplifies the analysis of the interference pattern, but also provides amplitudes with final states possessing definite CP-parities³. In order to determine the CP-parities associated to the different transversity amplitudes we follow the analysis of Ref. [35], where decays of the type $B \rightarrow MN$, with M, N unstable particles, are considered. The details of how to apply the results of Ref. [35] to the $B \rightarrow V\ell\ell$ decays of interest are provided in Appendix B; here we briefly summarize the main results.

We consider the decays $\bar{B} \rightarrow M_1 M_2 \ell^+ \ell^-$ and $\bar{B} \rightarrow \bar{M}_1 \bar{M}_2 \ell^+ \ell^-$, such that M_1, M_2 are either CP-eigenstates or CP-conjugates, and define the transversity amplitudes:

$$\bar{A}_X \equiv A_X(\bar{B} \rightarrow \bar{M}_1 \bar{M}_2 \ell^+ \ell^-), \quad \tilde{A}_X \equiv A_X(\bar{B} \rightarrow M_1 M_2 \ell^+ \ell^-), \quad (13)$$

where $X = L0, R0, L\parallel, R\parallel, L\perp, R\perp, t, S$. These two sets of amplitudes are related by

$$\tilde{A}_X = \eta_X \bar{A}_X \quad (14)$$

where η_X are the CP-parities associated to the different transversity amplitudes. We find that (see Appendix B)

$$\eta_X = \eta \quad \text{for } X = L0, L\parallel, R0, R\parallel, t; \quad \eta_X = -\eta \quad \text{for } X = L\perp, R\perp, S, \quad (15)$$

where $\eta = 1$ if M_1, M_2 are CP conjugates (e.g. $K^+ K^-$), and $\eta = -\eta(M_1)\eta(M_2)$ if M_1, M_2 are CP eigenstates (e.g. $K_S K_L$). Here $\eta(M)$ denotes the intrinsic CP-parity of meson M . For the three processes of interest mentioned in the introduction, the combination of intrinsic CP-parities leads always to $\eta = 1$.

At this point we can classify the angular observables J_i whether they combine amplitudes with identical or opposite CP-parities, and whether they involve real or imaginary parts of interference terms:

- Real part with identical CP-parities: $i = 1s, 1c, 2s, 2c, 3, 4$.
- Real part with opposite CP-parities: $i = 5, 6s, 6c$.
- Imaginary part with identical CP-parities: $i = 7$.
- Imaginary part with opposite CP-parities: $i = 8, 9$.

³We emphasise that the term ‘‘CP-parity’’ makes reference to the final states and not to the amplitudes themselves, since the latter involve either a B or a \bar{B} , which are not CP-eigenstates.

We note that the numbers ζ_i defined in Eq. (12) in a different context (identification of the kinematics between CP-conjugate decays) corresponds to the product of the CP-parities of the amplitudes involved in the interference term J_i .

We now turn to the case of decays into CP eigenstates: $B \rightarrow f_{CP}$. In this context, it is useful to define two different angular coefficients \tilde{J}_i , \bar{J}_i which are CP conjugates of J_i :

- the angular coefficients \tilde{J}_i formed by replacing A_X by $\tilde{A}_X \equiv A_X(\bar{B} \rightarrow f_{CP})$ (without CP-conjugation applied on f_{CP}), which appear naturally in the study of time evolution due to mixing, where both B and \bar{B} decay into the same final state f_{CP} .
- the angular coefficients \bar{J}_i , obtained by considering $\bar{A}_X \equiv A_X(\bar{B} \rightarrow \bar{f}_{CP})$ (with CP-conjugation applied to f_{CP}), which can be obtained from A_X by changing the sign of all weak phases, and arise naturally when discussing CP violation from the theoretical point of view.

From the discussion above we have $\tilde{A}_X = \eta_X \bar{A}_X$, with η_X given in Eq. (15). Plugging these amplitudes into the coefficients in Eq. (9), we see that the two types of angular coefficients are related through

$$\tilde{J}_i = \zeta_i \bar{J}_i, \quad (16)$$

with ζ_i given in Eq. (12). In addition, in the limit of CP conservation, $J_i = \bar{J}_i$.

Since the final state is not self-tagging, an untagged measurement of the differential decay rate (e.g. at LHCb, where the asymmetry production is tiny) yields essentially the CP-average

$$\frac{d\Gamma(B \rightarrow f_{CP}) + d\Gamma(\bar{B} \rightarrow f_{CP})}{ds \, d\cos\theta_\ell \, d\cos\theta_M \, d\phi} = \sum_i [J_i + \tilde{J}_i] f_i(\theta_\ell, \theta_M, \phi) = \sum_i [J_i + \zeta_i \bar{J}_i] f_i(\theta_\ell, \theta_M, \phi), \quad (17)$$

whereas the difference between the two decay rates (which can be measured only through flavour-tagging) involves $J_i - \tilde{J}_i = J_i - \zeta_i \bar{J}_i$,

$$\frac{d\Gamma(B \rightarrow f_{CP}) - d\Gamma(\bar{B} \rightarrow f_{CP})}{ds \, d\cos\theta_\ell \, d\cos\theta_M \, d\phi} = \sum_i [J_i - \tilde{J}_i] f_i(\theta_\ell, \theta_M, \phi) = \sum_i [J_i - \zeta_i \bar{J}_i] f_i(\theta_\ell, \theta_M, \phi). \quad (18)$$

We see that the convention chosen in Eqs. (10),(11) for flavour-tagging modes allows one to treat on the same footing these modes and the modes with final CP-eigenstates, since the same combinations of angular coefficients occur in both cases when one considers the CP-average or the CP-asymmetry in the decay rate. Let us add that this results from a conventional identification between CP-conjugate decays in the case without mixing. This freedom is not present in the presence of mixing where both decays result in the same final state, which must always be described with the “same” kinematic convention, in the sense of a convention that depends only on the final state, without referring to the flavour of the decaying B meson (see Appendix A).

A slightly counter-intuitive consequence is that the CP-asymmetries for J_i with $i = 5, 6s, 6c, 8, 9$ are measured in the CP-averaged rate, and vice-versa. We also note that due to the interferences between different decay amplitudes, only some of the $J_i - \bar{J}_i$ differences measure CP-violation in specific decay amplitudes (i.e., $|\bar{A}| = |A|$, $i = 1s, 1c, 2s, 2c, 3$) whereas the others measure relative phases between amplitudes ($i = 4, 5, 6s, 6c, 7, 8, 9$), see Eq. (9) .

2.3 Angular distributions in the presence of mixing

In the case of B decays into CP-eigenstates, where the final state can be produced both by the decay of B or \bar{B} mesons, the mixing and decay processes interfere, inducing a further time dependence in physical amplitudes (see e.g. Ref. [29, 34]). These time-dependent amplitudes are given by,

$$A_X(t) = A_X(B(t) \rightarrow V(\rightarrow f_{CP}) \rightarrow \ell^+ \ell^-) = g_+(t)A_X + \frac{q}{p}g_-(t)\tilde{A}_X , \quad (19)$$

$$\tilde{A}_X(t) = A_X(\bar{B}(t) \rightarrow V(\rightarrow f_{CP})\ell^+ \ell^-) = \frac{p}{q}g_-(t)A_X + g_+(t)\tilde{A}_X , \quad (20)$$

where the absence of the t argument denotes the amplitudes at $t = 0$, i.e. in the absence of mixing, and we have introduced the usual time-evolution functions

$$g_+(t) = e^{-imt}e^{-\Gamma t/2} \left[\cosh \frac{\Delta\Gamma t}{4} \cos \frac{\Delta m t}{2} - i \sinh \frac{\Delta\Gamma t}{4} \sin \frac{\Delta m t}{2} \right] , \quad (21)$$

$$g_-(t) = e^{-imt}e^{-\Gamma t/2} \left[-\sinh \frac{\Delta\Gamma t}{4} \cos \frac{\Delta m t}{2} + i \cosh \frac{\Delta\Gamma t}{4} \sin \frac{\Delta m t}{2} \right] , \quad (22)$$

with $\Delta m = M_H - M_L$ and $\Delta\Gamma = \Gamma_L - \Gamma_H$ (see Ref. [29]). The values of the different mixing parameters for the three decays of interest are collected in Table 1.

In the presence of mixing, the coefficients of the angular distribution also become time-dependent, as they depend on the time-dependent amplitudes in Eqs. (19),(20). This evolution can be simplified by noting that CP-violation in $B_q - \bar{B}_q$ mixing is negligible for all practical purposes⁴, and we will assume $|q/p| = 1$, introducing the mixing angle ϕ :

$$\frac{q}{p} = e^{i\phi} . \quad (23)$$

This mixing angle is large in the case of the B_d system but tiny for B_s , see Table 1.

The time-dependent angular coefficients are obtained by replacing time-independent amplitudes with time-dependent ones in Eqs. (9):

$$J_i(t) = J_i(A_X \rightarrow A_X(t)) , \quad \tilde{J}_i(t) = J_i(A_X \rightarrow \tilde{A}_X(t)) . \quad (24)$$

⁴The current world-averages are $|q/p|_{B_d} = 1.0007 \pm 0.0009$ and $|q/p|_{B_d} = 1.0038 \pm 0.0021$ [46].

Decay	η	ϕ	$\sin \phi$	$\cos \phi$	$\Delta\Gamma$	$x = \Delta m/\Gamma$	$y = \Delta\Gamma/(2\Gamma)$
$B_d \rightarrow K^{*0}(\rightarrow K_S \pi^0) \ell^+ \ell^-$	1	-2β	-0.7	0.7	$\simeq 0$	0.77	0
$B_s \rightarrow \phi(\rightarrow K_L K_S) \ell^+ \ell^-$	1	$2\beta_s$	0.04	1	$\neq 0$	27	0.06
$B_s \rightarrow \phi(\rightarrow K^+ K^-) \ell^+ \ell^-$	1	$2\beta_s$	0.04	1	$\neq 0$	27	0.06

Table 1: Parameters of the three decays of interest [46].

We consider the combinations $J_i(t) \pm \tilde{J}_i(t)$ appearing in the sum and difference of time-dependent decay rates in Eqs. (17), (18). From Eqs. (19), (20) and (24), we get

$$J_i(t) + \tilde{J}_i(t) = e^{-\Gamma t} \left[(J_i + \tilde{J}_i) \cosh(y\Gamma t) - h_i \sinh(y\Gamma t) \right], \quad (25)$$

$$J_i(t) - \tilde{J}_i(t) = e^{-\Gamma t} \left[(J_i - \tilde{J}_i) \cos(x\Gamma t) - s_i \sin(x\Gamma t) \right], \quad (26)$$

where $x \equiv \Delta m/\Gamma$, $y \equiv \Delta\Gamma/(2\Gamma)$, and we have defined a new set of angular coefficients s_i, h_i related to the time-dependent angular distribution. The coefficients J_i, \tilde{J}_i can already be determined from flavour-specific decays. The explicit expressions for s_i and h_i in terms of transversity amplitudes are collected in Appendix C.

Time-dependent angular distributions therefore contain potentially new information encoded in the new angular observables s_i and h_i . These pieces of information will be analysed in the rest of the paper. For the moment a few comments are in order:

- The coefficients h_i are very difficult to extract, since they are associated with $\sinh(y\Gamma t)$ with y very small. In particular, the time dependence of the untagged distribution (17) provides essentially no new information.
- The coefficients s_i for $i = 1s, 1c, 2s, 2c, 3, 4, 7$ are associated with a CP-asymmetry in angular coefficients: $J_i - \tilde{J}_i$.
- The coefficients s_i for $i = 5, 6s, 6c, 8, 9$ are associated with CP-averaged angular coefficients: $J_i + \tilde{J}_i$.
- The coefficients s_i for $i = 1s, 1c, 2s, 2c, 3, 4, 5, 6s, 6c$ are given by the imaginary part of amplitude interferences, $s_i \sim \text{Im}(e^{i\phi} \bar{A}_X A_Y^*)$, and vanish in the absence of complex phases. This is approximately true for $B_s \rightarrow V\ell\ell$ decays in the SM in regions where strong phases are small, e.g. in the region $s \simeq 1-6 \text{ GeV}^2$, and if the NP contribution has the same weak phase as the SM. The corresponding coefficients $J_i - \tilde{J}_i$ do not vanish, in general.
- The coefficient s_7 vanishes in the absence of phases in the amplitudes, while the combination $J_7 - \tilde{J}_7$ vanishes in the absence of CP violation in decay. Both are therefore very small in the SM, and also if the NP amplitudes have approximately the same phase as the SM.

- In the same conditions as above (no complex phases), the coefficients $(J_i + \bar{J}_i)_{i=8,9}$ vanish, while $s_{8,9}$ do not.

It seems therefore that the most promising observables in this context are $s_{8,9}$, which could be large and can be extracted from the time evolution of

$$J_8(t) - \tilde{J}_8(t) \simeq -s_8 e^{-\Gamma t} \sin(x\Gamma t) , \quad J_9(t) - \tilde{J}_9(t) \simeq -s_9 e^{-\Gamma t} \sin(x\Gamma t) . \quad (27)$$

The coefficients s_8 and s_9 have the following expressions (see Appendix C):

$$s_8 = -\frac{1}{\sqrt{2}} \beta_\ell^2 \text{Re} \left[e^{i\phi} (\bar{A}_0^L A_\perp^{L*} + \bar{A}_0^R A_\perp^{R*}) + e^{-i\phi} (A_0^L \bar{A}_\perp^{L*} + A_0^R \bar{A}_\perp^{R*}) \right] , \quad (28)$$

$$s_9 = \beta_\ell^2 \text{Re} \left[e^{i\phi} (\bar{A}_\parallel^L A_\perp^{L*} + \bar{A}_\parallel^R A_\perp^{R*}) + e^{-i\phi} (A_\parallel^L \bar{A}_\perp^{L*} + A_\parallel^R \bar{A}_\perp^{R*}) \right] . \quad (29)$$

We have checked by direct calculation that indeed the coefficients s_i with $i \neq 8, 9$ are tiny in the SM, and that they do not get significant enhancement from NP contributions if new sources of CP violation are not large.

We emphasise that the measurement of the coefficients $s_{8,9}$ is challenging from the experimental point of view, since the study of $J_i(t) - \tilde{J}_i(t)$ requires 1) flavour tagging of the original sample to separate B and \bar{B} at $t = 0$, 2) the use of appropriate foldings to extract the corresponding angular contributions, identical to the ones used to extract J_8 and J_9 [2,3], and 3) a time-dependent analysis to isolate the $\sin(x\Gamma t)$ coefficients.

2.4 Symmetries of the distribution

Having identified a few new observables accessible from the time-dependent angular distributions, it remains to be seen if they are truly independent from the observables that can be extracted from angular distributions of flavour-specific decays. The information that can be obtained from the angular distributions depends on the number of independent combinations of interference terms $A_X A_Y^*$ in the angular coefficients. A systematic formalism to determine which combinations can be accessed from the angular distributions alone is the “symmetry formalism” developed in Refs. [40, 47].⁵

In the approximation of massless leptons, and neglecting scalar and tensor operators, the angular distributions of flavour-specific decays contain a unitary symmetry, given by the transformation [40]:

$$n_i \equiv \begin{pmatrix} A_i^L \\ \sigma_i A_i^{R*} \end{pmatrix} \rightarrow U n_i \quad (30)$$

with U an arbitrary unitary 2×2 matrix, and $\{\sigma_0, \sigma_\parallel, \sigma_\perp\} \equiv \{1, 1, -1\}$. Under this group of transformations, $J_i \rightarrow J_i$. This means that from flavour-specific decays, only those combinations of terms $A_X A_Y^*$ that remain invariant under this transformation can

⁵See also Ref. [48] for an application to S- and P-wave components in $B \rightarrow (K\pi)\mu\mu$.

be accessed. This approach is useful to eliminate redundancies among observables built from the angular coefficients J_i [40, 47].

We now identify the transformation properties of the coefficients s_i –neglecting weak phases for simplicity. We note that, under the unitary transformation:

$$\begin{aligned} \text{Re}[A_i^L A_j^{L*} \pm A_i^R A_j^{R*}] &\longrightarrow [1 - (1 \mp \sigma_{ij})\lambda^2] \text{Re}[A_i^L A_j^{L*} \pm A_i^R A_j^{R*}] \\ &\quad + (1 \mp \sigma_{ij}) \text{Re}[\sigma_i \eta A_i^R A_j^L + \sigma_j \eta A_i^L A_j^R] , \end{aligned} \quad (31)$$

$$\begin{aligned} \text{Im}[A_i^L A_j^{L*} \pm A_i^R A_j^{R*}] &\longrightarrow [1 - (1 \pm \sigma_{ij})\lambda^2] \text{Im}[A_i^L A_j^{L*} \pm A_i^R A_j^{R*}] \\ &\quad - (1 \pm \sigma_{ij}) \text{Im}[\sigma_i \eta A_i^R A_j^L - \sigma_j \eta A_i^L A_j^R] , \end{aligned} \quad (32)$$

where $\sigma_{ij} = \sigma_i \sigma_j$, $\lambda^2 \equiv 1 - |U_{11}|^2$, $\eta \equiv U_{11} U_{12}^*$ and $i, j = 0, \parallel, \perp$. Non-trivial transformations involve only $\text{Re}[A_i^L A_j^{L*} \pm A_i^R A_j^{R*}]$ with $\sigma_{ij} = \mp 1$, or else $\text{Im}[A_i^L A_j^{L*} \pm A_i^R A_j^{R*}]$ with $\sigma_{ij} = \pm 1$. From the explicit expressions given in Appendix C, we see that (neglecting lepton mass terms and weak phases in the amplitudes):

$$s_{1s,2s} \sim \sin \phi \cdot \text{Re}[A_{\parallel}^L A_{\parallel}^{L*} + A_{\parallel}^R A_{\parallel}^{R*}] - (\parallel \rightarrow \perp) , \quad (33)$$

$$s_{1c,2c} \sim \sin \phi \cdot \text{Re}[A_0^L A_0^{L*} + A_0^R A_0^{R*}] , \quad (34)$$

$$s_3 \sim \sin \phi \cdot \text{Re}[A_{\parallel}^L A_{\parallel}^{L*} + A_{\parallel}^R A_{\parallel}^{R*}] + (\parallel \rightarrow \perp) , \quad (35)$$

$$s_4 \sim \sin \phi \cdot \text{Re}[A_0^L A_{\parallel}^{L*} + A_0^R A_{\parallel}^{R*}] , \quad (36)$$

$$s_5 \sim \cos \phi \cdot \text{Im}[A_0^L A_{\perp}^{L*} - A_0^R A_{\perp}^{R*}] , \quad (37)$$

$$s_{6s} \sim \cos \phi \cdot \text{Im}[A_{\parallel}^L A_{\perp}^{L*} - A_{\parallel}^R A_{\perp}^{R*}] , \quad (38)$$

$$s_7 \sim \sin \phi \cdot \text{Im}[A_0^L A_{\parallel}^{L*} - A_0^R A_{\parallel}^{R*}] , \quad (39)$$

$$s_8 \sim \cos \phi \cdot \text{Re}[A_0^L A_{\perp}^{L*} + A_0^R A_{\perp}^{R*}] , \quad (40)$$

$$s_9 \sim \cos \phi \cdot \text{Re}[A_{\parallel}^L A_{\perp}^{L*} + A_{\parallel}^R A_{\perp}^{R*}] . \quad (41)$$

Therefore the only coefficients s_i that (in this approximation) do not remain invariant are s_5 , s_{6s} , s_8 and s_9 , which contain additional information not accessible from the usual angular distributions of flavour-specific decays such as $B_d \rightarrow K^*(\rightarrow K^+ \pi^-) \ell \ell$. Among these coefficients, we have seen that $s_{8,9}$ are particularly promising; now we see that they are independent from the coefficients J_i .

3 Observables

The expressions in Eqs. (25), (26) for the coefficients of the time-dependent distributions, show that additional structures arise in the presence of neutral-meson mixing. In this context, two different quantities might be considered: time-integrated observables, or observables related to the time dependence. In this section we discuss the two possibilities.

3.1 Time-integrated observables

As discussed in Refs. [32,34], time integration should be performed differently in the context of hadronic machines and B -factories. The time-dependent expressions in Eqs. (25) and (26) are written in the case of tagging at a hadronic machine, assuming that the two b -quarks have been produced incoherently, with $t \in [0, \infty)$. In the case of a coherent $B\bar{B}$ pair produced at a B -factory, one must replace $\exp(-\Gamma t)$ by $\exp(-\Gamma|t|)$ and integrate over $t \in (-\infty, \infty)$ [34]. Interestingly, the integrated versions of CP-violating interference terms are different in both settings, and the measurement at hadronic machines involves an additional term compared to the B -factory case:

$$\langle J_i + \tilde{J}_i \rangle_{\text{Hadronic}} = \frac{1}{\Gamma} \left[\frac{1}{1-y^2} \times (J_i + \tilde{J}_i) - \frac{y}{1-y^2} \times h_i \right] , \quad (42)$$

$$\langle J_i - \tilde{J}_i \rangle_{\text{Hadronic}} = \frac{1}{\Gamma} \left[\frac{1}{1+x^2} \times (J_i - \tilde{J}_i) - \frac{x}{1+x^2} \times s_i \right] , \quad (43)$$

$$\langle J_i + \tilde{J}_i \rangle_{\text{B-factory}} = \frac{2}{\Gamma} \frac{1}{1-y^2} [J_i + \tilde{J}_i] , \quad (44)$$

$$\langle J_i - \tilde{J}_i \rangle_{\text{B-factory}} = \frac{2}{\Gamma} \frac{1}{1+x^2} [J_i - \tilde{J}_i] . \quad (45)$$

Making contact with experimental measurements requires to consider the total time-integrated decay rate. The time-dependent rate is given by

$$\frac{d\Gamma}{dq^2} = \int dt \left[\frac{3}{4} (2J_{1s}(t) + J_{1c}(t)) - \frac{1}{4} (2J_{2s}(t) + J_{2c}(t)) \right] , \quad (46)$$

which after time-integration becomes

$$\left\langle \frac{d\Gamma}{dq^2} \right\rangle = \frac{1}{\Gamma(1-y^2)} \langle \mathcal{I} \rangle , \quad (47)$$

$$\begin{aligned} \langle \mathcal{I} \rangle_{\text{Hadronic}} = & \frac{3}{4} \left[2(J_{1s} + \bar{J}_{1s} - y h_{1s}) + (J_{1c} + \bar{J}_{1c} - y h_{1c}) \right] \\ & - \frac{1}{4} \left[2(J_{2s} + \bar{J}_{2s} - y h_{2s}) + (J_{2c} + \bar{J}_{2c} - y h_{2c}) \right] , \end{aligned} \quad (48)$$

$$\langle \mathcal{I} \rangle_{B\text{-factory}} = \langle \mathcal{I} \rangle_{\text{Hadronic}}(h = 0) , \quad (49)$$

where \mathcal{I} is the usual normalisation considered in analyses of the angular coefficients. The normalised time-integrated angular coefficients at hadronic machines or B -factories are therefore:

$$\langle \Sigma_i \rangle_{\text{Hadronic}} \equiv \frac{\langle J_i + \tilde{J}_i \rangle_{\text{Hadronic}}}{\langle d\Gamma/dq^2 \rangle_{\text{Hadronic}}} = \frac{(J_i + \tilde{J}_i) - y \times h_i}{\langle \mathcal{I} \rangle_{\text{Hadronic}}} , \quad (50)$$

$$\langle \Sigma_i \rangle_{B\text{-factory}} \equiv \frac{\langle J_i + \tilde{J}_i \rangle_{B\text{-factory}}}{\langle d\Gamma/dq^2 \rangle_{B\text{-factory}}} = \langle \Sigma_i \rangle_{\text{Hadronic}}(h = 0) , \quad (51)$$

$$\langle \Delta_i \rangle_{\text{Hadronic}} \equiv \frac{\langle J_i - \tilde{J}_i \rangle_{\text{Hadronic}}}{\langle d\Gamma/dq^2 \rangle_{\text{Hadronic}}} = \frac{1 - y^2}{1 + x^2} \times \frac{(J_i - \tilde{J}_i) - x \times s_i}{\langle \mathcal{I} \rangle_{\text{Hadronic}}} , \quad (52)$$

$$\langle \Delta_i \rangle_{B\text{-factory}} \equiv \frac{\langle J_i - \tilde{J}_i \rangle_{B\text{-factory}}}{\langle d\Gamma/dq^2 \rangle_{B\text{-factory}}} = \langle \Delta_i \rangle_{\text{Hadronic}}(h = s = 0) . \quad (53)$$

We see that the interpretation of the time-integrated measurements $\langle \Sigma_i \rangle$ from $d\Gamma(B \rightarrow f_{CP}\ell\ell) + d\Gamma(\bar{B} \rightarrow f_{CP}\ell\ell)$ is straightforward in terms of the angular coefficients at $t = 0$. Even in the B_s case, the smallness of y means that h_i will have only a very limited impact on the discussion. The time-integrated terms $\langle \Delta_i \rangle$ from $d\Gamma(B \rightarrow f_{CP}\ell\ell) - d\Gamma(\bar{B} \rightarrow f_{CP}\ell\ell)$ are subject to two different effects, in particular for B_s where x is large:

- (a) they receive contributions proportional to x and y with a different combination of interference terms (in the case of a measurement at a hadronic machine),
- (b) they are suppressed (in all experimental set-ups) by a factor $(1 - y^2)/(1 + x^2)$.

The discussion above applies in particular to the measurement of $B_s \rightarrow \phi(\rightarrow K^+K^-)\ell\ell$ as performed at LHCb [12]. Since this is not a self-tagging mode, and assuming that there is an equal production of B_s and \bar{B}_s , what is measured is $d\Gamma(B_s \rightarrow \phi(\rightarrow K^+K^-)\ell\ell) + d\Gamma(\bar{B}_s \rightarrow \phi(\rightarrow K^+K^-)\ell\ell)$, so these measurements have access to the following combinations:

$$\begin{aligned} \langle J_i + \tilde{J}_i \rangle_{\text{Hadronic}} & \quad \text{for } i = 1s, 1c, 2s, 2c, 3, 4, 7, \\ \langle J_i - \tilde{J}_i \rangle_{\text{Hadronic}} & \quad \text{for } i = 5, 6s, 6c, 8, 9. \end{aligned} \quad (54)$$

The time-integrated observables $\langle \Sigma_6 \rangle_{\text{Hadronic}}$ and $\langle \Sigma_9 \rangle_{\text{Hadronic}}$ have already been measured (under the name of A_6 and A_9) in Ref. [12], and are indeed measuring CP-violation. In the context of the extraction of s_8 and s_9 at hadronic machines, one expects them to dominate $\langle \Delta_{8,9} \rangle_{\text{Hadronic}}$, especially in the case of B_s decays where x enhances their contribution with respect to the $(J_i - \tilde{J}_i)$ term. However, they are overall suppressed by a factor $\sim 1/x$, which in the case of B_s decays is quite effective ($1/x \sim 0.04$). In addition, the necessity to perform initial flavour tagging makes these measurements very difficult at hadronic machines.

We see therefore that $\langle \Sigma_i \rangle$ contain essentially the same information as $(J_i + \tilde{J}_i)$, whereas $\langle \Delta_i \rangle$ have a potentially richer interpretation, but are suppressed and thus probably difficult to extract experimentally. In the following section we will see that time-dependent observables do lead to more interesting opportunities.

3.2 Time-dependent “optimised” observables with tagging

From the discussion in Section 2.3 is clear that a full tagged time-dependent angular analysis of the decay $B \rightarrow V[\rightarrow (M_1 M_2)_{CP}] \ell \ell$ provides a measurement of the angular observables $J_i(s)$, $\bar{J}_i(s)$, $s_i(s)$ and $h_i(s)$, i.e. Eqs. (17), (18), (25), (26). We have also seen that the coefficients h_i are the $\sinh(y\Gamma t)$ coefficient of $J_i(t) + \tilde{J}_i(t)$, whose effect remains negligible for $t \lesssim 10 \tau_{B_q}$, constituting a rather difficult measurement.

From the theoretical point of view, these observables are quadratic in hadronic form factors (see Section 4.1). For instance,

$$s_i(s) \sim A_X A_Y^* \sim F_X^{B \rightarrow V}(s) \cdot F_Y^{B \rightarrow V}(s) , \quad (55)$$

and similarly for $J_i(s)$, $\bar{J}_i(s)$, $h_i(s)$. Here $F_{X,Y}$ represent (schematically) hadronic $B \rightarrow V$ form factors related to the amplitudes $A_{X,Y}$. These form factors constitute a major source of uncertainty in the theoretical predictions for the observables. This problem is usually tamed by defining a class of special observables with reduced sensitivity to form-factor uncertainties [40, 49–54]. These “optimised” observables can be constructed systematically, both in the region of large recoil of the vector meson ($s \ll m_B^2$) [40] and at low recoil ($s \sim m_B^2$) [50, 54], where the use of effective field theories (SCET [59, 60] and HQET [66, 67] respectively) ensures a complete cancellation of form factors at the leading order in the respective expansions⁶.

In the following, we focus on the large-recoil region for definiteness. We consider the following optimised versions of the observables $s_{8,9}$:

$$Q_8^- = \frac{s_8}{\sqrt{-2(J_{2c} + \tilde{J}_{2c})[2(J_{2s} + \tilde{J}_{2s}) - (J_3 + \tilde{J}_3)]}} , \quad (56)$$

$$Q_9 = \frac{s_9}{2(J_{2s} + \tilde{J}_{2s})} . \quad (57)$$

There are other possible normalizations for s_8 that are also optimised at large recoil:

$$Q_8^+ = \frac{s_8}{\sqrt{-2(J_{2c} + \tilde{J}_{2c})[2(J_{2s} + \tilde{J}_{2s}) + (J_3 + \tilde{J}_3)]}} , \quad (58)$$

⁶ In the following and throughout the paper we use the term “*large-recoil limit*” to denote the following approximation valid in the region $s \ll m_B^2$: leading order in α_s and leading power in the SCET expansion. This is, of course, a slight abuse of language.

$$Q_8^0 = \frac{s_8}{\sqrt{-2(J_{2c} + \tilde{J}_{2c})[2(J_{2s} + \tilde{J}_{2s})]}} . \quad (59)$$

The observable Q_8^+ has the particularity of being also optimised at low recoil. However, we find that both Q_8^+ and Q_8^0 are slightly less sensitive to NP than Q_8^- . While it might be worthwhile to study these observables further, we will focus here on Q_8^- for illustration, noting that its properties do not differ much from those of Q_8^+ , Q_8^0 .

Concerning Q_9 , other possible normalizations involve J_{6s} or J_9 , both of which lead to observables that are optimised also at low recoil. We do not consider these possibilities any further as the denominators contain zeroes within the kinematical region of interest.

It is useful to consider these observables in the large-recoil limit (see e.g. Refs. [40,41]), where the expressions simplify considerably, the cancellation of form factors is exact, and the dependence on the Wilson coefficients is apparent. We find:

$$Q_8^- = \left[\frac{\mathcal{C}_7^+(2\mathcal{C}_7^- + \mathcal{C}_9^-)}{2|\mathcal{C}_7^-|\sqrt{(\mathcal{C}_{10}^-)^2 + (2\mathcal{C}_7^- + \mathcal{C}_9^-)^2}} + \frac{(\mathcal{C}_{10}^-\mathcal{C}_{10}^+\mathcal{C}_7^- + (2\mathcal{C}_7^- + \mathcal{C}_9^-)(-\mathcal{C}_7^+\mathcal{C}_9^- + \mathcal{C}_7^-\mathcal{C}_9^+))}{4\mathcal{C}_7^-|\mathcal{C}_7^-|\sqrt{(\mathcal{C}_{10}^-)^2 + (2\mathcal{C}_7^- + \mathcal{C}_9^-)^2}} \frac{s}{m_B^2} + \dots \right] \cos \tilde{\phi}_q \quad (60)$$

$$Q_9 = - \left[\frac{2\mathcal{C}_7^-\mathcal{C}_7^+}{(\mathcal{C}_7^-)^2 + (\mathcal{C}_7^+)^2} + \frac{[(\mathcal{C}_7^-)^2 - (\mathcal{C}_7^+)^2](\mathcal{C}_7^-\mathcal{C}_9^+ - \mathcal{C}_7^+\mathcal{C}_9^-)}{[(\mathcal{C}_7^-)^2 + (\mathcal{C}_7^+)^2]^2} \frac{s}{m_B^2} + \dots \right] \cos \tilde{\phi}_q \quad (61)$$

where we have assumed real \mathcal{C}_i , and used the notation $\mathcal{C}_i^\pm = \mathcal{C}_i \pm \mathcal{C}_{i'}$. In the case of the $b \rightarrow s$ processes at hand, we have $\tilde{\phi}_q \equiv \phi_q - 2\beta_s$, with ϕ_q the mixing angle in the B_q system. We note that if $\mathcal{C}_{i'} = 0$ (that is, $\mathcal{C}_i^+ = \mathcal{C}_i^-$), one has $Q_9 = -\cos \tilde{\phi}_q$, so that the value of $(Q_9 + \cos \tilde{\phi}_q)$ is a measurement of right-handed currents.

In the following section we give Standard Model predictions for these observables and study briefly their sensitivity to New Physics.

4 Numerical Analysis

4.1 Standard Model

The systematic formalism to $B \rightarrow V\ell\ell$ decays at large hadronic recoil to NLO in QCD-factorisation has been presented in Ref. [55] and is by now quite standard. In our analysis we follow closely the procedure of Refs. [54,58] to which we refer the reader for further details. The different transversity amplitudes can be written as:

$$A_\perp^{L,R}(s) = \mathcal{N}_\perp \left\{ \left[(\mathcal{C}_9^+ + Y_t(s)(1 + \eta_{\text{PC}}^{(1)}) + \lambda_{ut}Y_u(s)) \mp \mathcal{C}_{10}^+ \right] \frac{V(s)}{M+m} + \frac{2m_b}{s} \mathcal{T}_1^+ \right\} , \quad (62)$$

$\mathcal{C}_1(\mu_b)$	$\mathcal{C}_2(\mu_b)$	$\mathcal{C}_3(\mu_b)$	$\mathcal{C}_4(\mu_b)$	$\mathcal{C}_5(\mu_b)$	$\mathcal{C}_6(\mu_b)$	$\mathcal{C}_7^{\text{eff}}(\mu_b)$	$\mathcal{C}_8^{\text{eff}}(\mu_b)$	$\mathcal{C}_9(\mu_b)$	$\mathcal{C}_{10}(\mu_b)$
-0.2632	1.0111	-0.0055	-0.0806	0.0004	0.0009	-0.2923	-0.1663	4.0749	-4.3085

Table 2: Wilson coefficients in the Standard Model at NNLO at the scale $\mu_b = 4.8 \text{ GeV}$.

$$A_{\parallel}^{L,R}(s) = \mathcal{N}_{\parallel} \left\{ \left[(\mathcal{C}_9^- + Y_t(s)(1 + \eta_{\text{PC}}^{(2)}) + \lambda_{ut} Y_u(s)) \mp \mathcal{C}_{10}^- \right] \frac{A_1(s)}{M + m} + \frac{2m_b}{s} \mathcal{T}_2^- \right\}, \quad (63)$$

$$A_0^{L,R}(s) = \mathcal{N}_0 \left\{ \left[(\mathcal{C}_9^- + Y_t(s)(1 + \eta_{\text{PC}}^{(3)}) + \lambda_{ut} Y_u(s)) \mp \mathcal{C}_{10}^- \right] \frac{A_{12}(s)}{M + m} + \frac{2m_b}{s} \left[(M^2 + 3m^2 - s) \mathcal{T}_2^- - \frac{\lambda}{M^2 - m^2} \mathcal{T}_3^- \right] \right\}, \quad (64)$$

$$A_t(s) = \frac{\mathcal{N}_{\perp}}{\sqrt{2}s} \left[2\mathcal{C}_{10}^- + \frac{s}{2m_{\ell}} \mathcal{C}_P^- \right] A_0(s), \quad A_S(s) = -\mathcal{N}_{\perp} \mathcal{C}_S^- A_0(s), \quad (65)$$

where $M = m_{B_q}$ and $m = m_V$, and:

- The normalizations are given by

$$\mathcal{N}_{\perp} = \sqrt{2\lambda} N, \quad \mathcal{N}_{\parallel} = \sqrt{2}(M^2 - m^2) N, \quad \mathcal{N}_0 = -N/(2m\sqrt{s}), \quad (66)$$

with $\lambda = M^4 + m^4 + s^2 - 2(M^2 m^2 + M^2 s + m^2 s)$, $\beta_{\ell} = \sqrt{1 - 4m_{\ell}^2/s}$, and

$$N(B) = V_{tb}^* V_{ts} \left[\frac{G_F^2 \alpha^2 s \lambda^{1/2} \beta_{\ell}}{3 \cdot 2^{10} \pi^5 M^3} \right]^{1/2}, \quad N(\bar{B}) = V_{tb} V_{ts}^* \left[\frac{G_F^2 \alpha^2 s \lambda^{1/2} \beta_{\ell}}{3 \cdot 2^{10} \pi^5 M^3} \right]^{1/2}. \quad (67)$$

- $Y_t(s)$ and $Y_u(s)$ are the 1-loop contributions from 4-quark operators to the photon penguin with the structure $\bar{s}\gamma_{\mu}b$, sometimes combined with \mathcal{C}_9 into $\mathcal{C}_{9\text{eff}}(s)$. $Y_t(s)$ denotes the contribution proportional to $V_{tb}V_{ts}^*$, and can be found in Eq.(10) of Ref. [55]. $Y_u(s)$ denotes the CKM-suppressed contribution, which is multiplied by the prefactor $\lambda_{ut}(B) = V_{ub}V_{us}^*/V_{tb}V_{ts}^*$ or $\lambda_{ut}(\bar{B}) = V_{ub}^*V_{us}/V_{tb}^*V_{ts}$. This function can be found in Eq. (A.3) of Ref. [56].
- The functions \mathcal{T}_i encode contributions from dipole operators $\mathcal{C}_{7(\nu)}$, and the rest of the hadronic contributions not contained in Y_t, Y_u :

$$\mathcal{T}_1^+(s) = \mathcal{C}_{7\text{eff}}^+ T_1(s) + \mathcal{T}_{\perp}(s)(1 + \eta_{\text{PC}}^{(1)}) \quad (68)$$

$$\mathcal{T}_2^-(s) = \mathcal{C}_{7\text{eff}}^- T_2(s) + \frac{M^2 - s}{M^2} \mathcal{T}_{\perp}(s)(1 + \eta_{\text{PC}}^{(2)}) \quad (69)$$

$$\mathcal{T}_3^-(s) = \mathcal{C}_{7\text{eff}}^- T_3(s) + \mathcal{T}_{\perp}(s) + \mathcal{T}_{\parallel}(s)(1 + \eta_{\text{PC}}^{(3)}) \quad (70)$$

The quantities $\mathcal{T}_{\perp, \parallel}$ represent factorizable and non-factorizable hadronic contributions in QCD-factorisation and can be extracted from the formulae in Section 2 of

Ref. [55]. They depend on distribution amplitudes and on two “soft” form factors $\xi_\perp(s)$, $\xi_\parallel(s)$. The “effective” coefficients $\mathcal{C}_{7\text{eff}}^\pm$ include contributions from 4-quark operators with b and s -quark loops with the structure $\bar{s}[\not{d}, \gamma_\mu]b$ (see e.g. Refs. [44, 57]).

- The parameters $\eta_{\text{PC}}^{(i)}$ in Eqs. (62)-(64) and (68)-(70) parametrize non-factorizable $\mathcal{O}(\Lambda/m_b)$ power corrections absent in the current QCD-factorisation calculation. Following Ref. [58], we write

$$\eta_{\text{PC}}^{(i)} = r_i^a e^{i\phi_i^a} + r_i^b e^{i\phi_i^b} (s/M^2) + r_i^c e^{i\phi_i^c} (s/M^2)^2 \quad (71)$$

and take $r_i^{a,b,c} = 0$ as our central value, varying the parameters r_i, ϕ_i within the ranges $r_i^{a,b,c} \in [0, 0.1]$ and $\phi_i^{a,b,c} \in [-\pi, \pi]$ in the error analysis. This corresponds to a contribution from non-factorizable $\mathcal{O}(\Lambda/m_b)$ corrections of $\mathcal{O}(10\%)$ with an arbitrary phase.

- The functions $V(s), A_0(s), A_1(s), A_2(s), T_1(s), T_2(s), T_3(s)$ represent the seven independent $B \rightarrow V$ QCD form factors (see e.g. Refs. [59, 60]), with the combination

$$A_{12}(s) = (M^2 - m^2 - s)(M + m)^2 A_1(s) - \lambda A_2(s) \quad (72)$$

entering $A_0^{L,R}$. Following Ref. [54], we use the large-recoil symmetry relations [59, 60] to express these form factors in terms of $\xi_\perp(s)$ and $\xi_\parallel(s)$, defined in the “scheme 1” of Ref. [58], including factorizable power corrections. At a second stage, these are themselves expressed in terms of $V(s), A_1(s), A_2(s)$, which are taken from the light-cone sum rule calculation of Ref. [61], both for $B \rightarrow K^*$ and $B_s \rightarrow \phi$ transitions.

- The Wilson coefficients \mathcal{C}_i^\pm are defined as: $\mathcal{C}_i^\pm = \mathcal{C}_i \pm \mathcal{C}_{i'}$. The Standard Model values for these coefficients are collected in Table 2, computed at a renormalisation scale $\mu_b = 4.8 \text{ GeV}$. As has become customary in analyses of $B \rightarrow V \ell \ell$ decays [18–25], we use NNLO Wilson coefficients, keeping in mind that the NNLO scheme and scale ambiguity can only be eliminated by including the (currently unknown) NNLO matrix elements. In this context, in the error analysis we consider a variation of the renormalisation scale $\mu \in [\mu_b/2, 2\mu_b]$. In addition, we have $\mathcal{C}_{7'}^{\text{SM}} = (m_s/m_b) \mathcal{C}_7^{\text{SM}}$.

Following this procedure, we compute central values and errors (by means of a flat scan over all parameters) for the observables Q_8^- and Q_9 in the SM. We compute these observables differentially in s , keeping in mind that a proper comparison with data would require an integration over bin ranges (see for example the discussion in Ref. [53]).

Our SM results for the observables Q_8^- and Q_9 in the low- s region are shown in Fig. 1. We show both cases: $B_s(t) \rightarrow \phi(\rightarrow KK)\mu^+\mu^-$ and $B_d(t) \rightarrow K^*(\rightarrow K_S\pi^0)\mu^+\mu^-$, noting that the results are very similar. We see that indeed the observable $Q_9 \simeq -\cos\tilde{\phi}_q$ in the whole region (with $\tilde{\phi}_d \simeq -2\beta$ and $\tilde{\phi}_s = 0$ in the SM), while Q_8^- features a distinctive

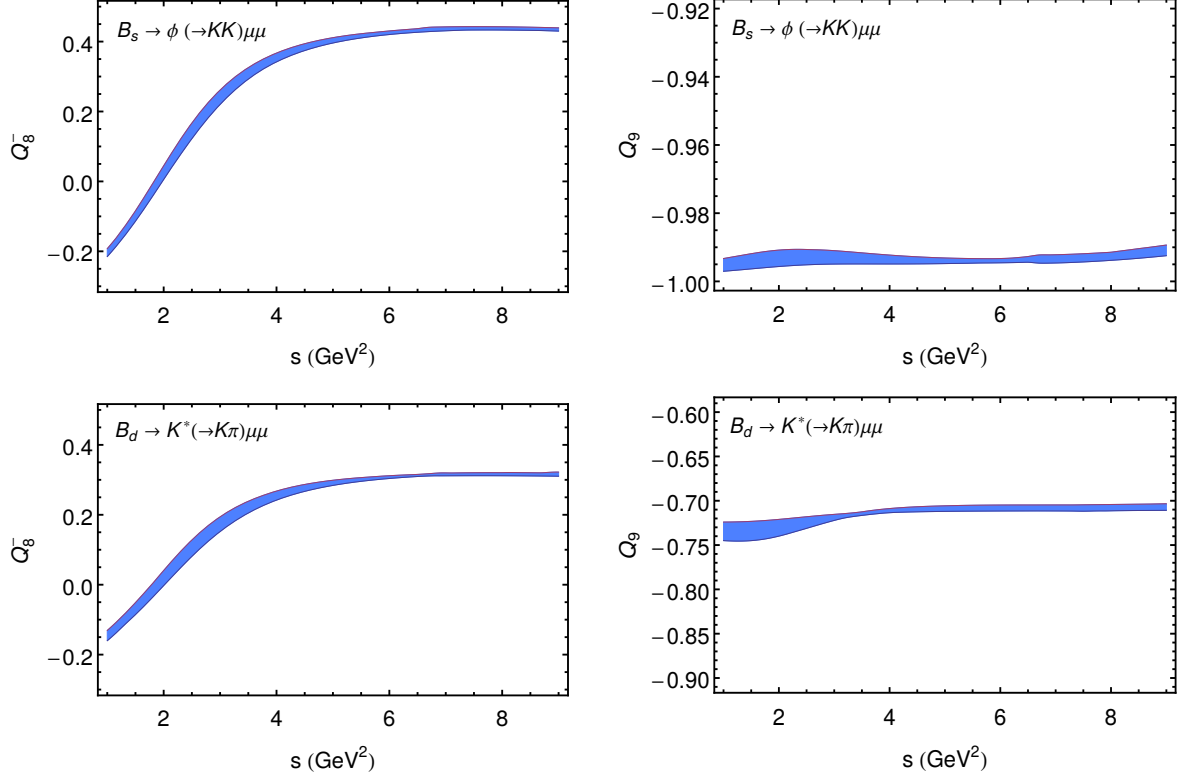


Figure 1: SM prediction for the observables Q_8^- and Q_9 in the case of $B_s(t) \rightarrow \phi(\rightarrow K^+ K^-) \mu^+ \mu^-$ (upper row) and $B_d(t) \rightarrow K^*(\rightarrow K_S \pi) \mu^+ \mu^-$ (lower row), in the large-recoil region, including error estimates from all sources. See the text for details.

shape with a zero at $s_0 \simeq 2 \text{ GeV}^2$. This is located at the same position as the zero of s_8 , which can be expressed solely in terms of Wilson coefficients taking the large-recoil limit,

$$\frac{s_0}{m_B^2} \simeq \frac{-2\mathcal{C}_7^+(2\mathcal{C}_7^- + \mathcal{C}_9^-)}{\mathcal{C}_{10}^-\mathcal{C}_{10}^+ + (2\mathcal{C}_7^- + \mathcal{C}_9^-)\mathcal{C}_9^+} \stackrel{\text{SM}}{\simeq} \frac{-2\mathcal{C}_7(2\mathcal{C}_7 + \mathcal{C}_9)}{\mathcal{C}_{10}^2 + (2\mathcal{C}_7 + \mathcal{C}_9)\mathcal{C}_9} . \quad (73)$$

The position of this zero measures a different ratio of Wilson coefficients compared to the zero of other observables, such as A_{FB} or P_2 [40]. We stress that the bands in Fig. 1 include all sources of error including parametric and form-factor uncertainties, as well as our estimates of power corrections, exhibiting the theoretical accuracy for these observables in the Standard Model.

4.2 New Physics

We now study the sensitivity of the observables Q_8^- and Q_9 to different models of New Physics. We start with a general scan of (real) New Physics contributions to Wilson coefficients compatible with all current constraints from rare B -decays, in order to assess the NP reach of the new observables. For that purpose, we write

$$\mathcal{C}_i = \mathcal{C}_i^{\text{SM}} + \mathcal{C}_i^{\text{NP}} , \quad (74)$$

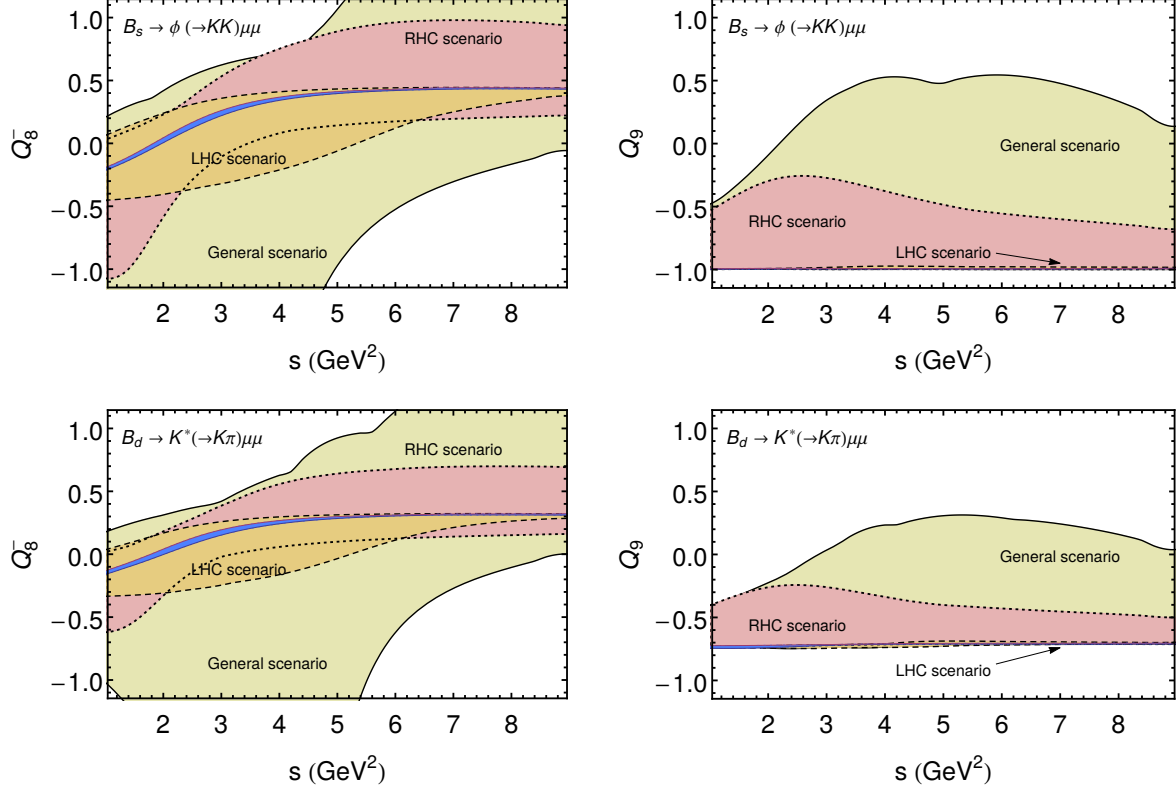


Figure 2: NP reach of the observables Q_8^- and Q_9 in the large-recoil region. See the text for details.

and consider the 3σ ranges for the NP contributions $\mathcal{C}_i^{\text{NP}}$ (at the scale $\mu_b = \mathcal{O}(m_b)$) that were obtained in the global fit to $b \rightarrow s\gamma$ and $b \rightarrow s\ell\ell$ data of Ref. [18]:

$$\begin{aligned} \mathcal{C}_7^{\text{NP}} &\in (-0.08, 0.03) , & \mathcal{C}_9^{\text{NP}} &\in (-2.1, -0.2) , & \mathcal{C}_{10}^{\text{NP}} &\in (-2.0, 3.0) , \\ \mathcal{C}_{7'}^{\text{NP}} &\in (-0.14, 0.10) , & \mathcal{C}_{9'}^{\text{NP}} &\in (-1.2, 1.8) , & \mathcal{C}_{10'}^{\text{NP}} &\in (-1.4, 1.2) . \end{aligned} \quad (75)$$

The result of this scan is shown in Fig. 2. We consider separately three scenarios:

- LHC (Left-Handed Currents) scenario: NP contributions to $\mathcal{C}_7, \mathcal{C}_9, \mathcal{C}_{10}$ only. This corresponds to the orange regions in Fig. 2, delimited by dashed lines (along the line $Q_9 = -1$ on the right-hand plot).
- RHC (Right-Handed Currents) scenario: NP contributions to $\mathcal{C}_{7'}, \mathcal{C}_{9'}, \mathcal{C}_{10'}$ only. This corresponds to the red regions in Fig. 2, delimited by dotted lines.
- General NP scenario: NP contributions to all six coefficients $\mathcal{C}_{7^{(\prime)}}, \mathcal{C}_{9^{(\prime)}}, \mathcal{C}_{10^{(\prime)}}$. This corresponds to the regions in green in Fig. 2, with solid borders.

We also show the SM predictions for comparison (blue bands in Fig. 2, with $Q_9^{\text{SM}} \simeq -1$ and $Q_9^{\text{SM}} \simeq -0.7$ for the B_s and B_d cases respectively). We see that NP can indeed have

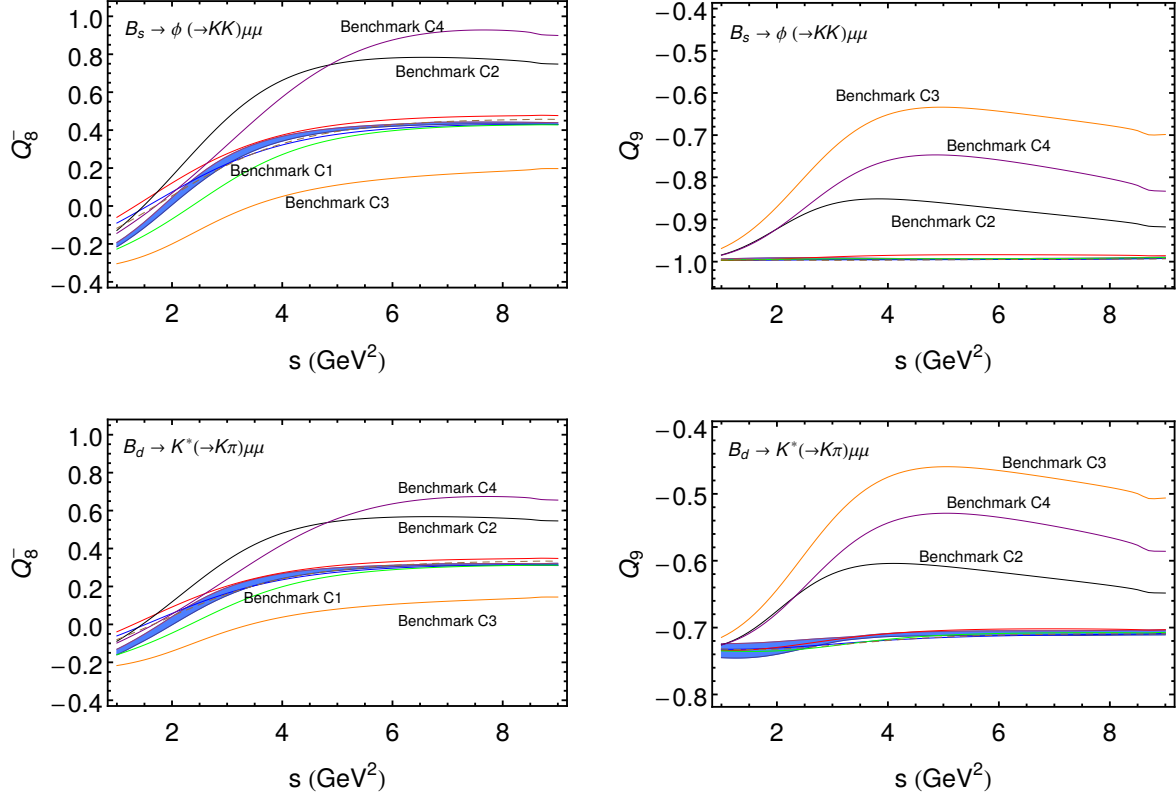


Figure 3: NP benchmarks for the observables Q_8^- and Q_9 in the large-recoil region. See the text for details. Benchmarks A (blue), B (red) and D (dashed) are hardly visible.

a large impact on Q_8^- , Q_9 . As discussed in Section 3.2, any significant deviation of Q_9 from $Q_9^{\text{SM}} \simeq -\cos \tilde{\phi}_q$ requires right-handed currents.

We finish our exploratory NP analysis by studying a few motivated benchmark NP scenarios:

A. Best fit point in the $\mathcal{C}_7 - \mathcal{C}_9$ scenario of Ref. [18]:

$$\mathcal{C}_7^{\text{NP}} = -0.02, \quad \mathcal{C}_9^{\text{NP}} = -1.6 .$$

B. Best fit point in the $\mathcal{C}_9 - \mathcal{C}_{9'}$ scenario of Ref. [25]:

$$\mathcal{C}_9^{\text{NP}} = -1.28, \quad \mathcal{C}_{9'}^{\text{NP}} = 0.47 .$$

C. Z' -motivated $\mathcal{C}_{9^{(\prime)}}$, $\mathcal{C}_{10^{(\prime)}}$ scenarios (see e.g. Refs. [62, 63]):

$$\text{C1. } \mathcal{C}_9^{\text{NP}} = -\mathcal{C}_{10}^{\text{NP}} = -1$$

$$\text{C2. } \mathcal{C}_{9'}^{\text{NP}} = -\mathcal{C}_{10'}^{\text{NP}} = 1$$

$$\text{C3. } \mathcal{C}_9^{\text{NP}} = \mathcal{C}_{9'}^{\text{NP}} = -\mathcal{C}_{10}^{\text{NP}} = -\mathcal{C}_{10'}^{\text{NP}} = -1$$

$$\text{C4. } \mathcal{C}_9^{\text{NP}} = -\mathcal{C}_{9'}^{\text{NP}} = -\mathcal{C}_{10}^{\text{NP}} = \mathcal{C}_{10'}^{\text{NP}} = -1$$

D. Best fit point in the general fit of Ref. [18]:

$$\mathcal{C}_7^{\text{NP}} = -0.02, \mathcal{C}_9^{\text{NP}} = -1.3, \mathcal{C}_{10}^{\text{NP}} = 0.3, \mathcal{C}_{7'}^{\text{NP}} = -0.01, \mathcal{C}_{9'}^{\text{NP}} = 0.3, \mathcal{C}_{10'}^{\text{NP}} = 0.$$

Scenarios C.1 and C.2 arise also respectively in singlet/triplet and doublet leptoquark models motivated by recent data on the ratio $\mathcal{B}(B \rightarrow K\mu\mu)/\mathcal{B}(B \rightarrow Kee)$ (see Ref. [22]).

The predictions for the observables Q_8^- and Q_9 within the benchmark scenarios are shown in Fig. 3, together with the SM prediction. We see that, among the considered scenarios, the only ones leading to significant deviations with respect to the SM are scenarios C (corresponding to large NP contributions to $\mathcal{C}_{9'}$ and $\mathcal{C}_{10'}$), while scenarios A, B and D are very close to the blue band (corresponding to the SM prediction). As discussed before, scenario C1 has no impact on Q_9 as it has no right-handed currents. Therefore, measurements of these observables compatible with the SM would give support to the best fit points obtained in the global fits of Ref. [18, 25] that we have considered, with the potential to exclude the scenarios with $\mathcal{C}_{9(\prime)}^{\text{NP}}, \mathcal{C}_{10(\prime)}^{\text{NP}}$ such as the one discussed in Ref. [22]. As an alternative viewpoint, these observables could test the latter scenarios, and provide an alternative confirmation if more accurate measurements for time-integrated observables happened to confirm any of them.

5 Conclusions

Decays of the type $B_{d,s} \rightarrow V(\rightarrow M_1 M_2)\ell^+\ell^-$ mediated by the underlying flavour-changing neutral current process $b \rightarrow s\ell\ell$ are of great phenomenological interest for two reasons: they lead to a vast set of independent experimental observables, and they exhibit a remarkable sensitivity to New Physics. The decay mode $B_d \rightarrow K^{*0}(\rightarrow K^-\pi^+)\mu^+\mu^-$ has been the first one to be carefully scrutinized, both experimentally [1–4, 7–11, 68] and theoretically [18–21, 69–111], and first angular analyses of the decays $B_s \rightarrow \phi(\rightarrow K^+K^-)\mu^+\mu^-$ [12] and $B_d \rightarrow K^{*0}(\rightarrow K^-\pi^+)e^+e^-$ [112] have been already performed.

In the case where $M_1 M_2$ is a CP eigenstate (such as $B_d \rightarrow K^{*0}(\rightarrow K_S\pi^0)\ell^+\ell^-$, $B_s \rightarrow \phi(\rightarrow K^+K^-)\mu^+\mu^-$ or $B_s \rightarrow \phi(\rightarrow K_S K_L)\mu^+\mu^-$), neutral B -meson mixing interferes with the decay, leading to interesting differences with respect to flavour-specific processes where mixing plays no role (such as $B_d \rightarrow K^{*0}(\rightarrow K^-\pi^+)\mu^+\mu^-$). In this paper we have studied the effects induced by neutral-meson mixing for the analysis of exclusive $B \rightarrow V\ell\ell$ decays, spelling out the theoretical formalism and analysing its phenomenological consequences.

As a first observation, the angular distributions become time-dependent, with additional structures compared to the case without mixing. These structures are the new angular coefficients h_i and s_i , defined in Eqs. (25),(26) and given explicitly in terms of the different amplitudes in Appendix C. Two types of observables can then be defined for these modes: time-integrated and time-dependent observables. The first type depend

on the experimental set-up (B -factory or hadronic machine) and differ from the corresponding observables in decays without mixing by multiplicative factors depending on the mixing parameters x and y . In addition, the expressions for time-integrated observables at hadronic machines include an extra term proportional to the coefficients h_i or s_i . This is similar to analogous relations derived for $B_s \rightarrow \phi(\rightarrow K^+K^-)\mu^+\mu^-$ [30], $B_s \rightarrow VV$ [32] and $B_s \rightarrow \mu^+\mu^-$ [31]. The corresponding expressions for time-integrated observables are given in Eqs. (42)-(45). However, it seems difficult to extract h_i or s_i using time-integrated observables, as they are suppressed by small meson-mixing parameters.

On the other hand, a time-dependent angular analysis with flavour tagging paves the way for the observables s_i . We identify s_8 and s_9 as the most interesting observables, as they are expected to be large even in the absence of CP violation. We have demonstrated that these observables contain new information compared to the angular coefficients J_i , and we have built “optimised” versions of these observables with reduced sensitivity to form factors. We have focused on two such observables, called Q_8^- and Q_9 and defined in Eqs. (56),(57). These observables can be predicted in the SM with good precision (see Fig. 1), and show good sensitivity to particular New Physics scenarios (see Figs. 2 and 3).

Current analyses of $b \rightarrow s\ell\ell$ transitions point towards deviations compared to SM expectations, explained via large NP contributions to \mathcal{C}_9 (and potentially smaller contributions to other Wilson coefficients). It is particularly interesting and useful to cross check this trend from other sources. Our analysis shows that additional information could come from time-dependent angular analyses of tagged $B_{d,s} \rightarrow V(\rightarrow M_1M_2)\ell\ell$ decays, with M_1M_2 a CP eigenstate. We thus encourage exploratory studies to determine the experimental feasibility of such analyses, in particular in the context of a high-luminosity flavour factory such as Belle-II.

Acknowledgements

We thank Damir Becirevic, Emi Kou, Quim Matias and Dirk Seidel for useful discussions. JV acknowledges the hospitality at LPT-Orsay where part of this work was done. JV is funded by the DFG within research unit FOR 1873 (QFET).

A CP-conjugate kinematics from invariants

The kinematics of the four-body decay $B \rightarrow V[\rightarrow M_1(p_1)M_2(p_2)]\ell^+(p_+)\ell^-(p_-)$, is completely specified by four invariant masses (e.g. $s_{+-} \equiv 2p_+ \cdot p_-$, $s_{1+} \equiv 2p_1 \cdot p_+$, $s_{1-} \equiv 2p_1 \cdot p_-$ and $s_{2+} \equiv 2p_2 \cdot p_+$), and the sign of $\epsilon_{12+-} \equiv \epsilon_{\mu\nu\rho\lambda}p_1^\mu p_2^\nu p_+^\rho p_-^\lambda$, which defines the parity of the final state [44]. We set these kinematic invariants to some fixed values s, s_1, s_2, s_3, σ such that:

$$s_{+-} = s, \quad s_{1+} = s_1, \quad s_{1-} = s_2, \quad s_{2+} = s_3, \quad \text{sgn}(\epsilon_{12+-}) = \sigma. \quad (76)$$

The kinematics of the CP-conjugated decay $\bar{B} \rightarrow \bar{V}[\rightarrow \bar{M}_1(p_{\bar{1}})\bar{M}_2(p_{\bar{2}})]\ell^+(p_+)\ell^-(p_-)$ is specified analogously. Under the condition of CP-conservation, the differential rates of both decays ($d\Gamma$ and $d\bar{\Gamma}$) must be equal at CP-conjugated kinematic points:

$$d\Gamma(s_{+-} = s, s_{1+} = s_1, s_{1-} = s_2, s_{2+} = s_3, \text{sgn}(\epsilon_{12+-}) = \sigma) \quad (77)$$

$$= d\bar{\Gamma}(s_{+-} = s, s_{\bar{1}-} = s_1, s_{\bar{1}+} = s_2, s_{\bar{2}-} = s_3, \text{sgn}(\epsilon_{\bar{1}\bar{2}-+}) = -\sigma)$$

$$= d\bar{\Gamma}(s_{+-} = s, s_{\bar{1}+} = s_2, s_{\bar{1}-} = s_1, s_{\bar{2}+} = m_B^2 - m_V^2 - s - s_1 - s_2 - s_3, \text{sgn}(\epsilon_{\bar{1}\bar{2}+-}) = \sigma),$$

where we have made the replacements $\{1, 2, +, -, \} \rightarrow \{\bar{1}, \bar{2}, -, +, \}$ and $\sigma \rightarrow -\sigma$ to account for C and P transformations respectively. In addition, we have used momentum conservation and neglected light-meson and lepton masses to write

$$s_{\bar{2}-} = m_B^2 - m_V^2 - s_{+-} - s_{\bar{1}+} - s_{\bar{1}-} - s_{\bar{2}+}. \quad (78)$$

The angular distribution is obtained by expressing these rates in terms of s_{+-} , two polar angles θ_M, θ_ℓ ($0 < \theta_i < \pi$), and one azimuthal angle⁷ ϕ ($0 < \phi < 2\pi$). In the case of $d\Gamma$, the angles are usually defined as [45]

- $\theta_M = \theta_1$: Polar angle between the momenta \vec{p}_B and \vec{p}_1 in the rest-frame of V . In terms of momentum invariants, we find:

$$\cos \theta_1 = \frac{m_B^2 - m_V^2 - s_{+-} - 2s_{1+} - 2s_{1-}}{\sqrt{(m_B^2 - m_V^2 - s_{+-})^2 - 4m_V^2 s_{+-}}} \equiv c_\theta(s_{+-}, s_{1+}, s_{1-}), \quad (79)$$

and $\sin \theta_1 = +\sqrt{1 - \cos^2 \theta_1}$ by definition.

- $\theta_\ell = \theta_+$: Polar angle between the momenta \vec{p}_B and \vec{p}_+ in the dilepton rest-frame. In terms of momentum invariants, we find:

$$\cos \theta_+ = \frac{m_B^2 - m_V^2 - s_{+-} - 2s_{1+} - 2s_{2+}}{\sqrt{(m_B^2 - m_V^2 - s_{+-})^2 - 4m_B^2 s_{+-}}} \equiv c_\theta(s_{+-}, s_{1+}, s_{2+}), \quad (80)$$

and again $\sin \theta_+ = +\sqrt{1 - \cos^2 \theta_+}$.

⁷ The kinematic angle ϕ should not be confused with the mixing angle, not appearing in this appendix.

- $\phi = \phi_{12+-}$: Oriented angle between the planes specified by (\vec{p}_1, \vec{p}_2) and (\vec{p}_+, \vec{p}_-) in the B -meson rest frame. The orientation is specified by (in this frame):

$$\cos \phi = \frac{(\vec{p}_1 \times \vec{p}_2) \cdot (\vec{p}_+ \times \vec{p}_-)}{|\vec{p}_1 \times \vec{p}_2| \cdot |\vec{p}_+ \times \vec{p}_-|}, \quad \sin \phi = \frac{(\vec{p}_+ + \vec{p}_-) \cdot [(\vec{p}_1 \times \vec{p}_2) \times (\vec{p}_+ \times \vec{p}_-)]}{|\vec{p}_+ + \vec{p}_-| \cdot |\vec{p}_1 \times \vec{p}_2| \cdot |\vec{p}_+ \times \vec{p}_-|}, \quad (81)$$

which in terms of momentum invariants gives:

$$\cos \phi_{12+-} = c_\phi(s, s_{1+}, s_{1-}, s_{2+}), \quad \sin \phi_{12+-} = \text{sgn}(\epsilon_{12+-}) \sqrt{1 - c_\phi^2}, \quad (82)$$

where $c_\phi(s, s_{1+}, s_{1-}, s_{2+}) = a/(2m_V b c)$ with

$$\begin{aligned} a &= m_V^4(s + s_{1+}) - (m_B^2 - s)[s_{1+}(-m_B^2 + s + s_{1-} + s_{1+}) + (s_{1-} + s_{1+})s_{2+}] + \\ &\quad m_V^2[s^2 - 2s_{1+} + (s_{1-} + s_{1+})(s_{1+} + s_{2+}) - s(m_B^2 - 2s_{1-} - 2s_{1+} - 2s_{2+})], \\ b &= \sqrt{s_{1-} + s_{1+} - (m_V^2 + s_{1-} + s_{1+})(s + s_{1-} + s_{1+})}, \\ c &= \sqrt{s[(s_{1+} + s_{2+})(m_B^2 - s - s_{1+} - s_{2+}) - m_V^2(s + s_{1+} + s_{2+})]}. \end{aligned} \quad (83)$$

We note that $\sin \phi$ is proportional to $\text{sign}(\epsilon_{12+-})$.

Other possibilities are $\theta_M = \theta_2$ or $\theta_\ell = \theta_-$, obtained from (79), (80) by obvious replacements. In the case of the CP-conjugate mode, the angles $\theta_{\bar{1}, \bar{2}}, \theta_\pm, \phi_{\bar{i}\bar{j}\pm\mp}$ are defined analogously.

In terms of the angular distribution, the CP correspondence in Eq. (77) depends on how the angles are defined for $d\bar{\Gamma}$, relative to $d\Gamma$. We recall that in the case of flavour-specific (“self-tagging”) modes, such as $B_d \rightarrow K^*(\rightarrow K^+\pi^-)\ell\ell$, one might choose any convention for $d\Gamma$ and $d\bar{\Gamma}$ independently, as the final states are different and distinguishable. However, this is not the case for untagged flavour-non-specific decays, where the final states arising from the B and the \bar{B} decay cannot be distinguished. We consider three different conventions:

- A.** $d\Gamma(s, \theta_1, \theta_+, \phi_{12+-})$ and $d\bar{\Gamma}(s, \theta_{\bar{1}}, \theta_+, \phi_{\bar{1}\bar{2}+-})$: This is the usual theory convention in $B_d \rightarrow K^*\ell\ell$, where in *both* CP-conjugated modes θ_M is defined with respect to the kaon, θ_ℓ with respect to the positively-charged lepton, and the orientation of ϕ is given by $\phi_{K\pi+-}$. This is also the only possible convention in untagged decays with $\bar{M}_1 = M_1$ and $\bar{M}_2 = M_2$, such as $B_d \rightarrow K^*(\rightarrow K_S\pi^0)\ell^+\ell^-$ and $B_s \rightarrow \phi(\rightarrow K_S K_L)\ell^+\ell^-$ at hadronic machines. With this convention, Eq. (77) implies

$$\begin{aligned} d\Gamma(s_{+-} = s, \cos \theta_1 = c_\theta(s, s_1, s_2), \cos \theta_+ = c_\theta(s, s_1, s_3), \\ \cos \phi = c_\phi(s, s_1, s_2, s_3), \text{sgn}(\sin \phi) = \sigma) = \end{aligned} \quad (84)$$

$$d\bar{\Gamma}(s_{+-} = s, \cos \theta_{\bar{1}} = c_{\theta}(s, s_2, s_1), \cos \theta_+ = c_{\theta}(s, s_2, m_B^2 - m_V^2 - s - s_1 - s_2 - s_3), \\ \cos \phi = c_{\phi}(s, s_2, s_1, m_B^2 - m_V^2 - s - s_1 - s_2 - s_3), \text{sgn}(\sin \phi) = \sigma)$$

We note the following relations:

$$c_{\theta}(s, s_1, s_2) \equiv X = c_{\theta}(s, s_2, s_1) , \quad (85)$$

$$c_{\theta}(s, s_1, s_3) \equiv Y = -c_{\theta}(s, s_2, m_B^2 - m_V^2 - s - s_1 - s_2 - s_3) , \quad (86)$$

$$c_{\phi}(s, s_1, s_2, s_3) \equiv Z = -c_{\phi}(s, s_2, s_1, m_B^2 - m_V^2 - s - s_1 - s_2 - s_3) . \quad (87)$$

Therefore,

$$d\Gamma(s_{+-} = s, \cos \theta_1 = X, \cos \theta_+ = Y, \cos \phi = Z, \text{sgn}(\sin \phi) = \sigma) = \\ d\bar{\Gamma}(s_{+-} = s, \cos \theta_{\bar{1}} = X, \cos \theta_+ = -Y, \cos \phi = -Z, \text{sgn}(\sin \phi) = \sigma) . \quad (88)$$

With the angles defined in this way, the two angular distributions are written as:

$$d\Gamma = \sum_i J_i(s) f_i(\theta_{\ell}, \theta_M, \phi) , \quad d\bar{\Gamma} = \sum_i \zeta_i \bar{J}_i(s) f_i(\theta_{\ell}, \theta_M, \phi) , \quad (89)$$

with $\zeta_{1,2,3,4,7} = 1$, $\zeta_{5,6,8,9} = -1$.

- B.** $d\Gamma(s, \theta_1, \theta_+, \phi_{12+-})$ and $d\bar{\Gamma}(s, \theta_{\bar{1}}, \theta_-, \phi_{\bar{1}\bar{2}+-})$: This is the usual experimental convention for $B_d \rightarrow K^* \ell \ell$, where in both modes $\theta_M = \theta_K$ and $\phi = \phi_{K\pi+-}$, but for θ_{ℓ} one takes ℓ^+ or ℓ^- for the B and \bar{B} decay respectively. We have:

$$d\Gamma(s_{+-} = s, \cos \theta_1 = c_{\theta}(s, s_1, s_2), \cos \theta_+ = c_{\theta}(s, s_1, s_3), \\ \cos \phi = c_{\phi}(s, s_1, s_2, s_3), \text{sgn}(\sin \phi) = \sigma) = \\ d\bar{\Gamma}(s_{+-} = s, \cos \theta_{\bar{1}} = c_{\theta}(s, s_2, s_1), \cos \theta_- = c_{\theta}(s, s_1, s_3), \\ \cos \phi = c_{\phi}(s, s_1, s_2, s_3), \text{sgn}(\sin \phi) = \sigma)$$

which means that, with this convention,

$$d\Gamma = \sum_i J_i(s) f_i(\theta_{\ell}, \theta_M, \phi) , \quad d\bar{\Gamma} = \sum_i \bar{J}_i(s) f_i(\theta_{\ell}, \theta_M, \phi) . \quad (91)$$

- C.** $d\Gamma(s, \theta_1, \theta_+, \phi_{12+-})$ and $d\bar{\Gamma}(s, \theta_{\bar{2}}, \theta_+, \phi_{\bar{2}\bar{1}+-})$: This is the only possible convention for the case of untagged decays where $\bar{M}_1 = M_2$ and $\bar{M}_2 = M_1$, as for example the decay $B_s \rightarrow \phi(\rightarrow K^+ K^-) \ell^+ \ell^-$ at a hadronic machine. In this case,

$$d\Gamma(s_{+-} = s, \cos \theta_1 = c_{\theta}(s, s_1, s_2), \cos \theta_+ = c_{\theta}(s, s_1, s_3), \\ \cos \phi = c_{\phi}(s, s_1, s_2, s_3), \text{sgn}(\sin \phi) = \sigma) =$$

$$\begin{aligned}
d\bar{\Gamma}(s_{+-} = s, \cos \theta_2 = c_\theta(s, m_B^2 - m_V^2 - s - s_1 - s_2 - s_3, s_3), \\
\cos \theta_+ = c_\theta(s, s_2, m_B^2 - m_V^2 - s - s_1 - s_2 - s_3), \\
\cos \phi = c_\phi(s, m_B^2 - m_V^2 - s - s_1 - s_2 - s_3, s_3, s_2), \text{sgn}(\sin \phi) = -\sigma) .
\end{aligned} \tag{92}$$

Using the relations

$$c_\theta(s, s_1, s_2) \equiv X = -c_\theta(s, m_B^2 - m_V^2 - s - s_1 - s_2 - s_3, s_3) , \tag{93}$$

$$c_\theta(s, s_1, s_3) \equiv Y = -c_\theta(s, s_2, m_B^2 - m_V^2 - s - s_1 - s_2 - s_3) , \tag{94}$$

$$c_\phi(s, s_1, s_2, s_3) \equiv Z = +c_\phi(s, m_B^2 - m_V^2 - s - s_1 - s_2 - s_3, s_3, s_2) , \tag{95}$$

we have

$$\begin{aligned}
d\Gamma(s_{+-} = s, \cos \theta_1 = X, \cos \theta_+ = Y, \cos \phi = Z, \text{sgn}(\sin \phi) = \sigma) = \\
d\bar{\Gamma}(s_{+-} = s, \cos \theta_2 = -X, \cos \theta_+ = -Y, \cos \phi = Z, \text{sgn}(\sin \phi) = -\sigma) .
\end{aligned} \tag{96}$$

With this convention, the differential rates are given by:

$$d\Gamma = \sum_i J_i(s) f_i(\theta_\ell, \theta_M, \phi) , \quad d\bar{\Gamma} = \sum_i \zeta_i \bar{J}_i(s) f_i(\theta_\ell, \theta_M, \phi) , \tag{97}$$

with $\zeta_{1,2,3,4,7} = 1$, $\zeta_{5,6,8,9} = -1$. This is the same as Eq. (89) but for a different reason.

We see that conventions A and C yield the same relation between $d\Gamma$ and $d\bar{\Gamma}$, but they apply to different kinds of modes. For decays into flavour-specific modes, convention B is also possible, but with a different relationship between $d\Gamma$ and $d\bar{\Gamma}$. In the present paper, we choose convention A for decays into flavour-specific modes as well as for $B \rightarrow V(\rightarrow M_1 M_2) \ell \ell$ decays with $\bar{M}_1 = M_1$, $\bar{M}_2 = M_2$, and convention C for $B \rightarrow V(\rightarrow M_1 M_2) \ell \ell$ decays with $\bar{M}_1 = M_2$, $\bar{M}_2 = M_1$.

B CP-parities associated to transversity amplitudes

We consider the decay $B \rightarrow VN$ (cf. Eq (4)) where V and N are unstable particles, V decaying into two particles M_1 and M_2 . As shown in Ref. [35], the CP-parity of a final state X is given by

$$\eta_X = \xi(-1)^\tau \tag{98}$$

with $\tau = \tau(M_1) + \tau(M_2) + \tau(N)$ the “transversity” of the state $M_1 M_2 N$ (defined below), and ξ depends on the class of decay:

- class 1: V (not necessarily with a definite spin) decays into M_1 and M_2 which are CP-eigenstates, and N decays into a CP-eigenstate. In this case,

$$\xi = \eta(N) \eta(M_1) \eta(M_2). \tag{99}$$

X	N	$\eta(N)$	s	$\tau(N)$	η_X
0	vector γ^*, Z (or axial) with ϵ_0	1	1	1	η
\parallel	vector γ^*, Z (or axial) with ϵ_{\parallel}	1	1	1	η
\perp	vector γ, Z (or axial) with ϵ_{\perp}	1	1	0	$-\eta$
S	scalar H	1	1	0	$-\eta$
t	vector γ^*, Z (or axial) with ϵ_t	-1	0	0	η
t	pseudoscalar A	-1	0	0	η

Table 3: Properties of the transversity amplitudes involved in $B \rightarrow V \ell \ell$: CP-parity of N , spin of the lepton pair, transversity of N , and CP-parity of the final state.

- class 2: V (with a definite spin s_V) decays into spin-0 M_1 and M_2 which are CP-conjugates, and N decays into a CP-eigenstate. In this case,

$$\xi = \eta(N)(-1)^{s_V}. \quad (100)$$

- class 3: V and N are CP-conjugates with a definite spin s_V , with V decaying into spin-0 M_1 and M_2 . In this case,

$$\xi = (-1)^{s_V}. \quad (101)$$

Here $\eta(V)$ and s_V are the intrinsic CP-parity and spin of the particle V . The first class is illustrated by the time-dependent analysis of $B_d \rightarrow J/\psi K^* (\rightarrow K_S \pi^0)$ [36]. For the class-1 processes ($B_d \rightarrow K^* (\rightarrow K_S \pi^0) \ell \ell$ and $B_s \rightarrow \phi (\rightarrow K_S K_L) \ell \ell$) and class-2 process ($B_s \rightarrow \phi (\rightarrow K^+ K^-) \ell \ell$) of interest, we have

$$\eta_X = \eta(N)(-1)^{\tau(N)+1} \eta \quad (102)$$

where $\eta = -\eta(M_1)\eta(M_2)$ for class-1, and $\eta = 1$ for class-2. For all the processes considered here, the combinations of intrinsic CP-parities yield $\eta = 1$.

In order to determine the CP-parity of the different transversity states, we have thus to determine $\eta(N)$ and $\tau(N)$:

- Using the language of Ref. [35], we see that $A_0, A_{\perp}, A_{\parallel}, A_{S,t}$ are respectively associated with the combinations of helicity amplitudes denoted $\mathcal{G}_{0,0,0}^{1+}, \mathcal{G}_{1,0,0}^{1+}, \mathcal{G}_{1,0,0}^{1-}, \mathcal{G}_{0,0,0}^{0+}$, with respective CP parities $-\xi, -\xi, \xi, \xi$. For our decays, it implies that we should have the following associations (modulo 2):

$$A_0, A_{\parallel} : \tau = 1, \quad A_{\perp}, A_t, A_S : \tau = 0 \quad (103)$$

The states corresponding to different transversities can be accessed through the angular analysis of the decay.

- $\eta(N)$ can be determined from the assumed quantum numbers of the intermediate boson (spin, polarisation, parity). $\eta(N)$ is identical for spin-1 particles with vector or axial couplings, whereas scalar and pseudoscalar N have opposite CP-parities. One can also notice that this constrains the spin of the emitted $\ell^+\ell^-$ pair. If we denote its angular momentum l and total spin s (either 0 or 1), the P -parity of such a fermion-antifermion pair is given by $(-1)^{l+1}$, its C parity by $(-1)^{l+s}$, so that its CP-parity is $(-1)^{s+1}$. Since we assumed that the decay $N \rightarrow \ell^+\ell^-$ conserves CP-parity, we have $\eta(N) = (-1)^{s+1}$. We have $l = s = 0$ corresponding to a pseudoscalar N , $l = s = 1$ corresponding to a scalar N , $l = 0, s = 1$ corresponding to a (real) vector/axial N , $l = 1, s = 0$ corresponding to a time-like vector/axial N (this can be checked from the CP-parity of the corresponding fermion-antifermion currents).

For each amplitude, we can determine the intermediate virtual boson N with the appropriate quantum numbers, the corresponding spin of the lepton pair, the transversity associated, and the CP-parity of the final state, as indicated in Table 3. We see in particular that we agree with the assignments for the class-1 decay $B_d \rightarrow J/\psi K^*(\rightarrow K_S \pi^0)$ [36]. In the end, we have

$$\eta_X = \eta \quad \text{for} \quad X = L0, L||, R0, R||, t \quad ; \quad \eta_X = -\eta \quad \text{for} \quad X = L \perp, R \perp, S. \quad (104)$$

We impose $\tau(N) = 0$ for a vector N with timelike polarisation, to obtain the same CP-parity as in the pseudoscalar case. This agrees with the expectation that A_t should have the same CP-parity as A_0 .

C Expressions for the coefficients s_i and h_i

The coefficients s_i are given by

$$s_{1s} = \frac{2 + \beta_\ell^2}{2} \text{Im}[e^{i\phi} \{ \tilde{A}_\perp^L A_\perp^{L*} + \tilde{A}_\parallel^L A_\parallel^{L*} + \tilde{A}_\perp^R A_\perp^{R*} + \tilde{A}_\parallel^R A_\parallel^{R*} \}] \\ + \frac{4m_\ell^2}{q^2} \text{Im}[e^{i\phi} \{ \tilde{A}_\perp^L A_\perp^{R*} + \tilde{A}_\parallel^L A_\parallel^{R*} \} - e^{-i\phi} \{ A_\perp^L \tilde{A}_\perp^{R*} + A_\parallel^L \tilde{A}_\parallel^{R*} \}] \quad (105)$$

$$s_{1c} = 2\text{Im}[e^{i\phi} \{ \tilde{A}_0^L A_0^{L*} + \tilde{A}_0^R A_0^{R*} \}] \\ + \frac{8m_\ell^2}{q^2} \left[\text{Im}[e^{i\phi} \{ \tilde{A}_t A_t^* \}] + \text{Im}[e^{i\phi} \tilde{A}_0^L A_0^{R*} - e^{-i\phi} A_0^L \tilde{A}_0^{R*}] \right] + 2\beta_\ell^2 \text{Im}[e^{i\phi} \tilde{A}_S A_S^*] \quad (106)$$

$$s_{2s} = \frac{\beta_\ell^2}{2} \text{Im}[e^{i\phi} \{ \tilde{A}_\perp^L A_\perp^{L*} + \tilde{A}_\parallel^L A_\parallel^{L*} + \tilde{A}_\perp^R A_\perp^{R*} + \tilde{A}_\parallel^R A_\parallel^{R*} \}] \quad (107)$$

$$s_{2c} = -2\beta_\ell^2 \text{Im}[e^{i\phi} \{ \tilde{A}_0^L A_0^{L*} + \tilde{A}_0^R A_0^{R*} \}] \quad (108)$$

$$s_3 = \beta_\ell^2 \text{Im}[e^{i\phi} \{ \tilde{A}_\perp^L A_\perp^{L*} - \tilde{A}_\parallel^L A_\parallel^{L*} + \tilde{A}_\perp^R A_\perp^{R*} - \tilde{A}_\parallel^R A_\parallel^{R*} \}] \quad (109)$$

$$s_4 = \frac{1}{\sqrt{2}}\beta_\ell^2 \text{Im}[e^{i\phi}\{\tilde{A}_0^L A_{||}^{L*} + \tilde{A}_0^R A_{||}^{R*}\} - e^{-i\phi}\{A_0^L \tilde{A}_{||}^{L*} + A_0^R \tilde{A}_{||}^{R*}\}] \quad (110)$$

$$s_5 = \sqrt{2}\beta_\ell \left[\text{Im}[e^{i\phi}\{\tilde{A}_0^L A_\perp^{L*} - \tilde{A}_0^R A_\perp^{R*}\} - e^{-i\phi}\{A_0^L \tilde{A}_\perp^{L*} - A_0^R \tilde{A}_\perp^{R*}\}] \right. \\ \left. - \frac{m_\ell}{\sqrt{q^2}} \text{Im}[e^{i\phi}\{\tilde{A}_{||}^L A_S^* + \tilde{A}_{||}^R A_S^*\} - e^{-i\phi}\{A_{||}^L \tilde{A}_S^* + A_{||}^R \tilde{A}_S^*\}] \right] \quad (111)$$

$$s_{6s} = 2\beta_\ell \text{Im}[e^{i\phi}\{\tilde{A}_{||}^L A_\perp^{L*} - \tilde{A}_{||}^R A_\perp^{R*}\} - e^{-i\phi}\{A_{||}^L \tilde{A}_\perp^{L*} - A_{||}^R \tilde{A}_\perp^{R*}\}] \quad (112)$$

$$s_{6c} = 4\beta_\ell \frac{m_\ell}{\sqrt{q^2}} \text{Im}[e^{i\phi}\{\tilde{A}_0^L A_S^* + \tilde{A}_0^R A_S^*\} - e^{-i\phi}\{A_0^L \tilde{A}_S^* + A_0^R \tilde{A}_S^*\}] \quad (113)$$

$$s_7 = -\sqrt{2}\beta_\ell \left[\text{Re}[e^{i\phi}\{\tilde{A}_0^L A_{||}^{L*} - \tilde{A}_0^R A_{||}^{R*}\} - e^{-i\phi}\{A_0^L \tilde{A}_{||}^{L*} - A_0^R \tilde{A}_{||}^{R*}\}] \right. \\ \left. + \frac{m_\ell}{\sqrt{q^2}} \text{Re}[e^{i\phi}\{\tilde{A}_\perp^L A_S^* + \tilde{A}_\perp^R A_S^*\} - e^{-i\phi}\{A_\perp^L \tilde{A}_S^* + A_\perp^R \tilde{A}_S^*\}] \right] \quad (114)$$

$$s_8 = -\frac{1}{\sqrt{2}}\beta_\ell^2 \text{Re}[e^{i\phi}\{\tilde{A}_0^L A_\perp^{L*} + \tilde{A}_0^R A_\perp^{R*}\} - e^{-i\phi}\{A_0^L \tilde{A}_\perp^{L*} + A_0^R \tilde{A}_\perp^{R*}\}] \quad (115)$$

$$s_9 = \beta_\ell^2 \text{Re}[e^{i\phi}\{\tilde{A}_{||}^L A_\perp^{L*} + \tilde{A}_{||}^R A_\perp^{R*}\} - e^{-i\phi}\{A_{||}^L \tilde{A}_\perp^{L*} + A_{||}^R \tilde{A}_\perp^{R*}\}] \quad (116)$$

The coefficients h_i are given by

$$h_{1s} = \frac{2 + \beta_\ell^2}{2} \text{Re}[e^{i\phi}\{\tilde{A}_\perp^L A_\perp^{L*} + \tilde{A}_{||}^L A_{||}^{L*} + \tilde{A}_\perp^R A_\perp^{R*} + \tilde{A}_{||}^R A_{||}^{R*}\}] \\ + \frac{4m_\ell^2}{q^2} \text{Re}[e^{i\phi}\{\tilde{A}_\perp^L A_\perp^{R*} + \tilde{A}_{||}^L A_{||}^{R*}\} + e^{-i\phi}\{A_\perp^L \tilde{A}_\perp^{R*} + A_{||}^L \tilde{A}_{||}^{R*}\}] \quad (117)$$

$$h_{1c} = 2\text{Re}[e^{i\phi}\{\tilde{A}_0^L A_0^{L*} + \tilde{A}_0^R A_0^{R*}\}] \\ + \frac{8m_\ell^2}{q^2} [\text{Re}[e^{i\phi}\tilde{A}_t A_t^*] + \text{Re}\{e^{i\phi}\tilde{A}_0^L A_0^{R*} + e^{-i\phi}A_0^L \tilde{A}_0^{R*}\}] + 2\beta_\ell^2 \text{Re}[e^{i\phi}\{\tilde{A}_S A_S^*\}] \quad (118)$$

$$h_{2s} = \frac{\beta_\ell^2}{2} \text{Re}[e^{i\phi}\{\tilde{A}_\perp^L A_\perp^{L*} + \tilde{A}_{||}^L A_{||}^{L*} + \tilde{A}_\perp^R A_\perp^{R*} + \tilde{A}_{||}^R A_{||}^{R*}\}] \quad (119)$$

$$h_{2c} = -2\beta_\ell^2 \text{Re}[e^{i\phi}\{\tilde{A}_0^L A_0^{L*} + \tilde{A}_0^R A_0^{R*}\}] \quad (120)$$

$$h_3 = \beta_\ell^2 \text{Re}[e^{i\phi}\{\tilde{A}_\perp^L A_\perp^{L*} - \tilde{A}_{||}^L A_{||}^{L*} + \tilde{A}_\perp^R A_\perp^{R*} - \tilde{A}_{||}^R A_{||}^{R*}\}] \quad (121)$$

$$h_4 = \frac{1}{\sqrt{2}}\beta_\ell^2 \text{Re}[e^{i\phi}\{\tilde{A}_0^L A_{||}^{L*} + \tilde{A}_0^R A_{||}^{R*}\} + e^{-i\phi}\{A_0^L \tilde{A}_{||}^{L*} + A_0^R \tilde{A}_{||}^{R*}\}] \quad (122)$$

$$h_5 = \sqrt{2}\beta_\ell \left[\text{Re}[e^{i\phi}\{\tilde{A}_0^L A_\perp^{L*} - \tilde{A}_0^R A_\perp^{R*}\} + e^{-i\phi}\{A_0^L \tilde{A}_\perp^{L*} - A_0^R \tilde{A}_\perp^{R*}\}] \right. \quad (123)$$

$$\left. - \frac{m_\ell}{\sqrt{q^2}} \text{Re}[e^{i\phi}\{\tilde{A}_\parallel^L A_S^* + \tilde{A}_\parallel^R A_S^*\} + e^{-i\phi}\{A_\parallel^L \tilde{A}_S^* + A_\parallel^R \tilde{A}_S^*\}] \right]$$

$$h_{6s} = 2\beta_\ell \text{Re}[e^{i\phi}\{\tilde{A}_\parallel^L A_\perp^{L*} - \tilde{A}_\parallel^R A_\perp^{R*}\} + e^{-i\phi}\{A_\parallel^L \tilde{A}_\perp^{L*} - A_\parallel^R \tilde{A}_\perp^{R*}\}] \quad (124)$$

$$h_{6c} = 4\beta_\ell \frac{m_\ell}{\sqrt{q^2}} \text{Re}[e^{i\phi}\{\tilde{A}_0^L A_S^* + \tilde{A}_0^R A_S^*\} + e^{-i\phi}\{A_0^L \tilde{A}_S^* + A_0^R \tilde{A}_S^*\}] \quad (125)$$

$$h_7 = \sqrt{2}\beta_\ell \left[\text{Im}[e^{i\phi}\{\tilde{A}_0^L A_\parallel^{L*} - \tilde{A}_0^R A_\parallel^{R*}\} + e^{-i\phi}\{A_0^L \tilde{A}_\parallel^{L*} - A_0^R \tilde{A}_\parallel^{R*}\}] \right. \quad (126)$$

$$\left. + \frac{m_\ell}{\sqrt{q^2}} \text{Im}[e^{i\phi}\{\tilde{A}_\perp^L A_S^* + \tilde{A}_\perp^R A_S^*\} + e^{-i\phi}\{A_\perp^L \tilde{A}_S^* + A_\perp^R \tilde{A}_S^*\}] \right]$$

$$h_8 = \frac{1}{\sqrt{2}}\beta_\ell^2 \text{Im}[e^{i\phi}\{\tilde{A}_0^L A_\perp^{L*} + \tilde{A}_0^R A_\perp^{R*}\} + e^{-i\phi}\{A_0^L \tilde{A}_\perp^{L*} + A_0^R \tilde{A}_\perp^{R*}\}] \quad (127)$$

$$h_9 = -\beta_\ell^2 \text{Im}[e^{i\phi}\{\tilde{A}_\parallel^L A_\perp^{L*} + \tilde{A}_\parallel^R A_\perp^{R*}\} + e^{-i\phi}\{A_\parallel^L \tilde{A}_\perp^{L*} + A_\parallel^R \tilde{A}_\perp^{R*}\}] \quad (128)$$

In the above expressions, the amplitude \tilde{A}_X denotes the amplitude $A_X(\bar{B} \rightarrow f)$, without applying CP-conjugation to the final state. One has the relation

$$\tilde{A}_X = \eta_X \bar{A}_X \quad (129)$$

where \bar{A}_X can be obtained from A_X by changing the sign of all weak phases.

References

- [1] **Babar** Collaboration, J. L. Ritchie, “Angular Analysis of $B \rightarrow K^* \ell^+ \ell^-$ in BABAR,” arXiv:1301.1700 [hep-ex].
- [2] **LHCb** Collaboration, “Differential branching fraction and angular analysis of the decay $B^0 \rightarrow K^{*0} \mu^+ \mu^-$,” JHEP **1308**, 131 (2013), arXiv:1304.6325[hep-ex].
- [3] **LHCb** Collaboration, “Measurement of Form-Factor-Independent Observables in the Decay $B^0 \rightarrow K^{*0} \mu^+ \mu^-$,” Phys. Rev. Lett. **111**, no. 19, 191801 (2013), arXiv:1308.1707 [hep-ex].
- [4] **CMS** Collaboration, “Angular analysis and branching fraction measurement of the decay $B^0 \rightarrow K^{*0} \mu^+ \mu^-$,” Phys. Lett. B **727**, 77 (2013), arXiv:1308.3409 [hep-ex].

- [5] **LHCb** Collaboration, “Angular analysis of charged and neutral $B \rightarrow K\mu^+\mu^-$ decays,” JHEP **1405**, 082 (2014), arXiv:1403.8045 [hep-ex].
- [6] **LHCb** Collaboration, “Test of lepton universality using $B^+ \rightarrow K^+\ell^+\ell^-$ decays,” Phys. Rev. Lett. **113**, no. 15, 151601 (2014), arXiv:1406.6482 [hep-ex].
- [7] **Belle** Collaboration, “Measurement of the Differential Branching Fraction and Forward-Backward Asymmetry for $B \rightarrow K^{(*)}\ell^+\ell^-$,” Phys. Rev. Lett. **103**, 171801 (2009), arXiv:0904.0770 [hep-ex].
- [8] **CDF** Collaboration, “Measurements of the Angular Distributions in the Decays $B \rightarrow K^{(*)}\mu^+\mu^-$ at CDF,” Phys. Rev. Lett. **108**, 081807 (2012), arXiv:1108.0695 [hep-ex].
- [9] **Babar** Collaboration, “Measurement of Branching Fractions and Rate Asymmetries in the Rare Decays $B \rightarrow K^{(*)}l^+l^-$,” Phys. Rev. D **86**, 032012 (2012), arXiv:1204.3933 [hep-ex].
- [10] **LHCb** Collaboration, “Differential branching fractions and isospin asymmetries of $B \rightarrow K^{(*)}\mu^+\mu^-$ decays,” JHEP **1406**, 133 (2014), arXiv:1403.8044 [hep-ex].
- [11] **LHCb** Collaboration, “Measurement of CP asymmetries in the decays $B^0 \rightarrow K^{*0}\mu^+\mu^-$ and $B^+ \rightarrow K^+\mu^+\mu^-$,” JHEP **1409**, 177 (2014), arXiv:1408.0978 [hep-ex].
- [12] **LHCb** Collaboration, “Differential branching fraction and angular analysis of the decay $B_s^0 \rightarrow \phi\mu^+\mu^-$,” JHEP **1307**, 084 (2013), arXiv:1305.2168 [hep-ex].
- [13] **LHCb** Collaboration, “Measurement of the $B_s^0 \rightarrow \mu^+\mu^-$ branching fraction and search for $B^0 \rightarrow \mu^+\mu^-$ decays at the LHCb experiment,” Phys. Rev. Lett. **111**, 101805 (2013), arXiv:1307.5024 [hep-ex].
- [14] **CMS** Collaboration, “Measurement of the $B_s \rightarrow \mu^+\mu^-$ branching fraction and search for $B^0 \rightarrow \mu^+\mu^-$ with the CMS Experiment,” Phys. Rev. Lett. **111**, 101804 (2013), arXiv:1307.5025 [hep-ex].
- [15] F. Archilli, “ $B_s^0 \rightarrow \mu^+\mu^-$ at LHC,” arXiv:1411.4964 [hep-ex].
- [16] **Babar** Collaboration, “Measurement of the $B \rightarrow X_s\ell^+\ell^-$ branching fraction and search for direct CP violation from a sum of exclusive final states,” Phys. Rev. Lett. **112**, 211802 (2014), arXiv:1312.5364 [hep-ex].
- [17] **Belle** Collaboration, “Measurement of the Lepton Forward-Backward Asymmetry in Inclusive $B \rightarrow X_s\ell^+\ell^-$ Decays,” arXiv:1402.7134 [hep-ex].
- [18] S. Descotes-Genon, J. Matias and J. Virto, “Understanding the $B \rightarrow K^*\mu^+\mu^-$ Anomaly,” Phys. Rev. D **88**, no. 7, 074002 (2013), arXiv:1307.5683 [hep-ph].

- [19] W. Altmannshofer and D. M. Straub, “New physics in $B \rightarrow K^* \mu \mu$?,” Eur. Phys. J. C **73**, no. 12, 2646 (2013), arXiv:1308.1501 [hep-ph].
- [20] F. Beaujean, C. Bobeth and D. van Dyk, “Comprehensive Bayesian analysis of rare (semi)leptonic and radiative B decays,” Eur. Phys. J. C **74**, no. 6, 2897 (2014) [Erratum-ibid. C **74**, no. 12, 3179 (2014)] [arXiv:1310.2478 [hep-ph].
- [21] R. R. Horgan, Z. Liu, S. Meinel and M. Wingate, “Calculation of $B^0 \rightarrow K^{*0} \mu^+ \mu^-$ and $B_s^0 \rightarrow \phi \mu^+ \mu^-$ observables using form factors from lattice QCD,” Phys. Rev. Lett. **112**, 212003 (2014), arXiv:1310.3887 [hep-ph].
- [22] G. Hiller and M. Schmaltz, “ R_K and future $b \rightarrow s \ell \ell$ physics beyond the standard model opportunities,” Phys. Rev. D **90**, no. 5, 054014 (2014), arXiv:1408.1627 [hep-ph].
- [23] D. Ghosh, M. Nardecchia and S. A. Renner, “Hint of Lepton Flavour Non-Universality in B Meson Decays,” JHEP **1412**, 131 (2014), arXiv:1408.4097 [hep-ph].
- [24] T. Hurth, F. Mahmoudi and S. Neshatpour, “Global fits to $b \rightarrow s \ell \ell$ data and signs for lepton non-universality,” JHEP **1412**, 053 (2014), arXiv:1410.4545 [hep-ph].
- [25] W. Altmannshofer and D. M. Straub, “State of new physics in $b \rightarrow s$ transitions,” arXiv:1411.3161 [hep-ph].
- [26] S. L. Glashow, D. Guadagnoli and K. Lane, “Lepton Flavor Violation in B Decays?,” arXiv:1411.0565 [hep-ph].
- [27] B. Gripaios, M. Nardecchia and S. A. Renner, “Composite leptoquarks and anomalies in B -meson decays,” arXiv:1412.1791 [hep-ph].
- [28] B. Bhattacharya, A. Datta, D. London and S. Shivashankara, “Simultaneous Explanation of the R_K and $R(D^{(*)})$ Puzzles,” arXiv:1412.7164 [hep-ph].
- [29] U. Nierste, “Three Lectures on Meson Mixing and CKM phenomenology,” arXiv:0904.1869 [hep-ph].
- [30] C. Bobeth, G. Hiller and G. Piranishvili, “CP Asymmetries in $\bar{B} \rightarrow \bar{K}^*(\rightarrow \bar{K} \pi) \bar{\ell} \ell$ and Untagged $\bar{B}_s, B_s \rightarrow \phi(\rightarrow K^+ K^-) \bar{\ell} \ell$ Decays at NLO,” JHEP **0807** (2008) 106, arXiv:0805.2525 [hep-ph].
- [31] K. De Bruyn, R. Fleischer, R. Knegjens, P. Koppenburg, M. Merk, A. Pellegrino and N. Tuning, “Probing New Physics via the $B_s^0 \rightarrow \mu^+ \mu^-$ Effective Lifetime,” Phys. Rev. Lett. **109**, 041801 (2012), arXiv:1204.1737 [hep-ph].
- [32] S. Descotes-Genon, J. Matias and J. Virto, “An analysis of $B_{d,s}$ mixing angles in presence of New Physics and an update of $B_s \rightarrow K^{0*} \bar{K}^{0*}$,” Phys. Rev. D **85**, 034010 (2012), arXiv:1111.4882 [hep-ph].

- [33] **Belle-II** Collaboration, T. Abe *et al.* “Belle II Technical Design Report,” arXiv:1011.0352 [physics.ins-det].
- [34] **Babar** Collaboration, P. F. Harrison *et al.* “The BABAR physics book: Physics at an asymmetric B factory,” SLAC-R-0504.
- [35] I. Dunietz, H. R. Quinn, A. Snyder, W. Toki and H. J. Lipkin, “How to extract CP violating asymmetries from angular correlations,” Phys. Rev. D **43** (1991) 2193.
- [36] **Babar** Collaboration, “Ambiguity-free measurement of $\cos(2\beta)$: Time-integrated and time-dependent angular analyses of $B \rightarrow J/\psi K\pi$,” Phys. Rev. D **71** (2005) 032005 [hep-ex/0411016].
- [37] P. Ball and R. Zwicky, “Time-dependent CP Asymmetry in $B \rightarrow K^*\gamma$ as a (Quasi) Null Test of the Standard Model,” Phys. Lett. B **642** (2006) 478 [hep-ph/0609037].
- [38] F. Muheim, Y. Xie and R. Zwicky, “Exploiting the width difference in $B_s \rightarrow \phi\gamma$,” Phys. Lett. B **664** (2008) 174, arXiv:0802.0876 [hep-ph].
- [39] W. Altmannshofer, P. Ball, A. Bharucha, A. J. Buras, D. M. Straub and M. Wick, “Symmetries and Asymmetries of $B \rightarrow K^*\mu^+\mu^-$ Decays in the Standard Model and Beyond,” JHEP **0901** (2009) 019, arXiv:0811.1214 [hep-ph].
- [40] J. Matias, F. Mescia, M. Ramon, J. Virto, “Complete Anatomy of $\bar{B}_d \rightarrow \bar{K}^{*0}(\rightarrow K\pi)\ell^+\ell^-$ and its angular distribution,” JHEP **1204** (2012) 104, arXiv:1202.4266 [hep-ph].
- [41] S. Descotes-Genon, D. Ghosh, J. Matias and M. Ramon, “Exploring New Physics in the $\mathcal{C}_7\text{-}\mathcal{C}_7'$ plane,” JHEP **1106** (2011) 099, arXiv:1104.3342 [hep-ph].
- [42] S. Jäger, J. Martin Camalich, “On $B \rightarrow V\ell\ell$ at small dilepton invariant mass, power corrections, and new physics,” JHEP **1305**, 043 (2013), arXiv:1212.2263 [hep-ph].
- [43] K. G. Chetyrkin, M. Misiak and M. Munz, “Weak radiative B meson decay beyond leading logarithms,” Phys. Lett. B **400**, 206 (1997) [Erratum-ibid. B **425**, 414 (1998)] [hep-ph/9612313].
- [44] T. Huber, M. Poradziński and J. Virto, “Four-body contributions to $\bar{B} \rightarrow X_s\gamma$ at NLO,” JHEP **1501**, 115 (2015), arXiv:1411.7677 [hep-ph].
- [45] F. Kruger, L. M. Sehgal, N. Sinha and R. Sinha, “Angular distribution and CP asymmetries in the decays $\bar{B} \rightarrow K^-\pi^+e^-e^+$ and $\bar{B} \rightarrow \pi^-\pi^+e^-e^+$,” Phys. Rev. D **61**, 114028 (2000) [Erratum-ibid. D **63**, 019901 (2001)] [hep-ph/9907386].
- [46] **HFAG** Collaboration, Y. Amhis *et al.*, “Averages of b -hadron, c -hadron, and τ -lepton properties as of summer 2014,” arXiv:1412.7515 [hep-ex].

- [47] U. Egede, T. Hurth, J. Matias, M. Ramon and W. Reece, “New physics reach of the decay mode $\bar{B} \rightarrow \bar{K}^{*0} \ell^+ \ell^-$,” JHEP **1010**, 056 (2010), arXiv:1005.0571 [hep-ph].
- [48] L. Hofer and J. Matias, “Exploiting the Symmetries of P and S wave for $B \rightarrow K^* \mu^+ \mu^-$,” arXiv:1502.00920 [hep-ph].
- [49] F. Kruger and J. Matias, “Probing new physics via the transverse amplitudes of $\bar{B}^0 \rightarrow K^{*0}(\rightarrow K^- \pi^+) \ell^+ \ell^-$ at large recoil,” Phys. Rev. D **71**, 094009 (2005) [hep-ph/0502060].
- [50] C. Bobeth, G. Hiller and D. van Dyk, “The Benefits of $\bar{B} \rightarrow \bar{K}^* \ell^+ \ell^-$ Decays at Low Recoil,” JHEP **1007**, 098 (2010), arXiv:1006.5013 [hep-ph].
- [51] C. Bobeth, G. Hiller and D. van Dyk, “More Benefits of Semileptonic Rare B Decays at Low Recoil: CP Violation,” JHEP **1107**, 067 (2011), arXiv:1105.0376 [hep-ph].
- [52] D. Becirevic and E. Schneider, “On transverse asymmetries in $B \rightarrow K^* \ell^+ \ell^-$,” Nucl. Phys. B **854**, 321 (2012), arXiv:1106.3283 [hep-ph].
- [53] S. Descotes-Genon, J. Matias, M. Ramon and J. Virto, “Implications from clean observables for the binned analysis of $B \rightarrow K^* \mu^+ \mu^-$ at large recoil,” JHEP **1301**, 048 (2013), arXiv:1207.2753 [hep-ph].
- [54] S. Descotes-Genon, T. Hurth, J. Matias and J. Virto, “Optimizing the basis of $B \rightarrow K^* \ell^+ \ell^-$ observables in the full kinematic range,” JHEP **1305**, 137 (2013), arXiv:1303.5794 [hep-ph].
- [55] M. Beneke, T. Feldmann and D. Seidel, “Systematic approach to exclusive $B \rightarrow V \ell^+ \ell^-, V \gamma$ decays,” Nucl. Phys. B **612**, 25 (2001) [hep-ph/0106067].
- [56] M. Beneke, T. Feldmann and D. Seidel, “Exclusive radiative and electroweak $b \rightarrow d$ and $b \rightarrow s$ penguin decays at NLO,” Eur. Phys. J. C **41**, 173 (2005) [hep-ph/0412400].
- [57] K. G. Chetyrkin, M. Misiak and M. Munz, “ $\Delta F = 1$ nonleptonic effective Hamiltonian in a simpler scheme,” Nucl. Phys. B **520**, 279 (1998) [hep-ph/9711280].
- [58] S. Descotes-Genon, L. Hofer, J. Matias and J. Virto, “On the impact of power corrections in the prediction of $B \rightarrow K^* \mu^+ \mu^-$ observables,” JHEP **1412**, 125 (2014), arXiv:1407.8526 [hep-ph].
- [59] J. Charles, A. Le Yaouanc, L. Oliver, O. Pene and J. C. Raynal, “Heavy to light form-factors in the heavy mass to large energy limit of QCD,” Phys. Rev. D **60**, 014001 (1999) [hep-ph/9812358].
- [60] M. Beneke and T. Feldmann, “Symmetry breaking corrections to heavy to light B meson form-factors at large recoil,” Nucl. Phys. B **592**, 3 (2001) [hep-ph/0008255].

- [61] P. Ball and R. Zwicky, “ $B_{d,s} \rightarrow \rho, \omega, K^*, \phi$ decay form-factors from light-cone sum rules revisited,” Phys. Rev. D **71**, 014029 (2005) [hep-ph/0412079].
- [62] A. J. Buras, F. De Fazio and J. Girrbach, “The Anatomy of Z' and Z with Flavour Changing Neutral Currents in the Flavour Precision Era,” JHEP **1302**, 116 (2013), arXiv:1211.1896 [hep-ph].
- [63] A. J. Buras and J. Girrbach, “Left-handed Z' and Z FCNC quark couplings facing new $b \rightarrow s\mu^+\mu^-$ data,” JHEP **1312**, 009 (2013), arXiv:1309.2466 [hep-ph].
- [64] J. Brod, A. Lenz, G. Tetlalmatzi-Xolocotzi and M. Wiebusch, “New physics effects in tree-level decays,” arXiv:1412.1446 [hep-ph].
- [65] A. Faessler, T. Gutsche, M. A. Ivanov, J. G. Korner and V. E. Lyubovitskij, “The Exclusive rare decays $B \rightarrow K(K^*)\bar{\ell}\ell$ and $B_c \rightarrow D(D^*)\bar{\ell}\ell$ in a relativistic quark model,” Eur. Phys. J. direct C **4**, 18 (2002) [hep-ph/0205287].
- [66] B. Grinstein and D. Pirjol, “Exclusive rare $B \rightarrow K^*\ell^+\ell^-$ decays at low recoil: Controlling the long-distance effects,” Phys. Rev. D **70**, 114005 (2004) [hep-ph/0404250].
- [67] M. Beylich, G. Buchalla and T. Feldmann, “Theory of $B \rightarrow K^{(*)}\ell^+\ell^-$ decays at high q^2 : OPE and quark-hadron duality,” Eur. Phys. J. C **71**, 1635 (2011), arXiv:1101.5118 [hep-ph].
- [68] T. Blake, T. Gershon and G. Hiller, “Rare b hadron decays at the LHC,” arXiv:1501.03309 [hep-ex].
- [69] D. Das and R. Sinha, “New Physics Effects and Hadronic Form Factor Uncertainties in $B \rightarrow K^*\ell^+\ell^-$,” Phys. Rev. D **86**, 056006 (2012), arXiv:1205.1438 [hep-ph].
- [70] F. Beaujean, C. Bobeth, D. van Dyk and C. Wacker, “Bayesian Fit of Exclusive $b \rightarrow s\bar{\ell}\ell$ Decays: The Standard Model Operator Basis,” JHEP **1208**, 030 (2012), arXiv:1205.1838 [hep-ph].
- [71] F. Mahmoudi, S. Neshatpour, J. Orloff, “Supersymmetric constraints from $B_s \rightarrow \mu^+\mu^-$ and $B \rightarrow K^*\mu^+\mu^-$ observables,” JHEP **1208**, 092 (2012), arXiv:1205.1845 [hep-ph].
- [72] A. Y. Korchin and V. A. Kovalchuk, “Contribution of vector resonances to the $\bar{B}_d^0 \rightarrow \bar{K}^{*0}\mu^+\mu^-$ decay,” Eur. Phys. J. C **72**, 2155 (2012), arXiv:1205.3683 [hep-ph].
- [73] W. Altmannshofer and D. M. Straub, “Cornering New Physics in $b \rightarrow s$ Transitions,” JHEP **1208**, 121 (2012), arXiv:1206.0273 [hep-ph].
- [74] N. Kosnik, “Model independent constraints on leptoquarks from $b \rightarrow s\ell^+\ell^-$ processes,” Phys. Rev. D **86**, 055004 (2012), arXiv:1206.2970 [hep-ph].

- [75] D. Becirevic and A. Tayduganov, “Impact of $B \rightarrow K_0^* \ell^+ \ell^-$ on the New Physics search in $B \rightarrow K^* \ell^+ \ell^-$ decay,” Nucl. Phys. B **868**, 368 (2013), arXiv:1207.4004 [hep-ph].
- [76] S. Descotes-Genon, J. Matias and J. Virto, “New Physics constraints from optimized observables in $B \rightarrow K^* \ell^+ \ell^-$ at large recoil,” AIP Conf. Proc. **1492**, 103 (2012), arXiv:1209.0262 [hep-ph].
- [77] J. Matias, “On the S-wave pollution of $B \rightarrow K^* \ell^+ \ell^-$ observables,” Phys. Rev. D **86**, 094024 (2012), arXiv:1209.1525 [hep-ph].
- [78] T. Blake, U. Egede and A. Shires, “The effect of S-wave interference on the $B^0 \rightarrow K^{*0} \ell^+ \ell^-$ angular observables,” JHEP **1303**, 027 (2013), arXiv:1210.5279 [hep-ph].
- [79] T. Hurth and F. Mahmoudi, “Colloquium: New physics search with flavor in the LHC era,” Rev. Mod. Phys. **85**, 795 (2013), arXiv:1211.6453 [hep-ph].
- [80] C. Bobeth, G. Hiller and D. van Dyk, “General analysis of $\bar{B} \rightarrow \bar{K}^{(*)} \ell^+ \ell^-$ decays at low recoil,” Phys. Rev. D **87**, no. 3, 034016 (2013), arXiv:1212.2321 [hep-ph].
- [81] H. Gong, Y. D. Yang and X. B. Yuan, “Constraints on anomalous tcZ coupling from $\bar{B} \rightarrow \bar{K}^* \mu^+ \mu^-$ and $B_s \rightarrow \mu^+ \mu^-$ decays,” JHEP **1305**, 062 (2013), arXiv:1301.7535 [hep-ph].
- [82] S. Descotes-Genon, T. Hurth, J. Matias and J. Virto, “ $B \rightarrow K^* \ell \ell$: The New Frontier of New Physics searches in Flavor,” arXiv:1305.4808 [hep-ph].
- [83] A. J. Buras and J. Girrbach, “Towards the Identification of New Physics through Quark Flavour Violating Processes,” Rept. Prog. Phys. **77**, 086201 (2014) arXiv:1306.3775 [hep-ph].
- [84] R. Gauld, F. Goertz, U. Haisch, “On minimal Z' explanations of the $B \rightarrow K^* \mu^+ \mu^-$ anomaly,” Phys. Rev. D **89**, no. 1, 015005 (2014), arXiv:1308.1959 [hep-ph].
- [85] C. Hambrock, G. Hiller, S. Schacht, R. Zwicky, “ $B \rightarrow K^*$ form factors from flavor data to QCD and back,” Phys. Rev. D **89**, 074014 (2014), arXiv:1308.4379 [hep-ph].
- [86] R. Gauld, F. Goertz and U. Haisch, “An explicit Z' -boson explanation of the $B \rightarrow K^* \mu^+ \mu^-$ anomaly,” JHEP **1401**, 069 (2014), arXiv:1310.1082 [hep-ph].
- [87] A. Datta, M. Duraissamy and D. Ghosh, “Explaining the $B \rightarrow K^* \mu^+ \mu^-$ data with scalar interactions,” Phys. Rev. D **89**, no. 7, 071501 (2014), arXiv:1310.1937 [hep-ph].
- [88] R. R. Horgan, Z. Liu, S. Meinel and M. Wingate, “Lattice QCD calculation of form factors describing the rare decays $B \rightarrow K^* \ell^+ \ell^-$ and $B_s \rightarrow \phi \ell^+ \ell^-$,” Phys. Rev. D **89**, no. 9, 094501 (2014), arXiv:1310.3722 [hep-lat].

- [89] S. Descotes-Genon, J. Matias and J. Virto, “Optimizing the basis of $B \rightarrow K^* l^+ l^-$ observables and understanding its tensions,” PoS EPS **-HEP2013**, 361 (2013), arXiv:1311.3876 [hep-ph].
- [90] A. J. Buras, F. De Fazio and J. Girrbach, “331 models facing new $b \rightarrow s \mu^+ \mu^-$ data,” JHEP **1402**, 112 (2014), arXiv:1311.6729 [hep-ph].
- [91] G. Hiller and R. Zwicky, “(A)symmetries of weak decays at and near the kinematic endpoint,” JHEP **1403**, 042 (2014), arXiv:1312.1923 [hep-ph].
- [92] T. Hurth and F. Mahmoudi, “On the LHCb anomaly in $B \rightarrow K^* \ell^+ \ell^-$,” JHEP **1404**, 097 (2014), arXiv:1312.5267 [hep-ph].
- [93] F. Mahmoudi, S. Neshatpour and J. Virto, “ $B \rightarrow K^* \mu^+ \mu^-$ optimised observables in the MSSM,” Eur. Phys. J. C **74**, no. 6, 2927 (2014), arXiv:1401.2145 [hep-ph].
- [94] M. Ahmady, R. Campbell, S. Lord and R. Sandapen, “Predicting the $B \rightarrow K^*$ form factors in light-cone QCD,” Phys. Rev. D **89**, no. 7, 074021 (2014), arXiv:1401.6707 [hep-ph].
- [95] G. Isidori and F. Teubert, “Status of indirect searches for New Physics with heavy flavour decays after the initial LHC run,” Eur. Phys. J. Plus **129**, 40 (2014), arXiv:1402.2844 [hep-ph].
- [96] J. Matias and N. Serra, “Symmetry relations between angular observables in $B^0 \rightarrow K^* \mu^+ \mu^-$ and the LHCb P'_5 anomaly,” Phys. Rev. D **90**, no. 3, 034002 (2014), arXiv:1402.6855 [hep-ph].
- [97] W. Altmannshofer, S. Gori, M. Pospelov and I. Yavin, “Quark flavor transitions in $L_\mu - L_\tau$ models,” Phys. Rev. D **89**, no. 9, 095033 (2014), arXiv:1403.1269 [hep-ph].
- [98] P. Biancofiore, P. Colangelo and F. De Fazio, “Rare semileptonic $B \rightarrow K^* \ell^+ \ell^-$ decays in RS_c model,” Phys. Rev. D **89**, no. 9, 095018 (2014), arXiv:1403.2944 [hep-ph].
- [99] A. J. Buras, F. De Fazio and J. Girrbach-Noe, “ Z - Z' mixing and Z -mediated FCNCs in $SU(3)_C \times SU(3)_L \times U(1)_X$ models,” JHEP **1408**, 039 (2014), arXiv:1405.3850 [hep-ph].
- [100] W. Altmannshofer, “New Physics Interpretations of the $B \rightarrow K^* \mu^+ \mu^-$ Anomaly,” arXiv:1405.5182 [hep-ph].
- [101] J. Lyon and R. Zwicky, “Resonances gone topsy turvy - the charm of QCD or new physics in $b \rightarrow s \ell^+ \ell^-$?,” arXiv:1406.0566 [hep-ph].
- [102] M. R. Ahmady, S. Lord and R. Sandapen, “Isospin asymmetry in $B \rightarrow K^* \mu^+ \mu^-$ using AdS/QCD,” Phys. Rev. D **90**, no. 7, 074010 (2014), arXiv:1407.6700 [hep-ph].

- [103] S. Sun, “Little Flavor: Heavy Leptons, Z' and Higgs Phenomenology,” arXiv:1411.0131 [hep-ph].
- [104] S. Descotes-Genon, L. Hofer, J. Matias and J. Virto, “QCD uncertainties in the prediction of $B \rightarrow K^* \mu^+ \mu^-$ observables,” arXiv:1411.0922 [hep-ph].
- [105] H. B. Fu, X. G. Wu and Y. Ma, “ $B \rightarrow K^*$ Transition Form Factors and the Semi-leptonic Decay $B \rightarrow K^* \mu^+ \mu^-$,” arXiv:1411.6423 [hep-ph].
- [106] M. Blanke, “Flavour Physics Beyond the Standard Model: Recent Developments and Future Perspectives,” arXiv:1412.1003 [hep-ph].
- [107] G. Kumar and N. Mahajan, “ $B \rightarrow K^* l^+ l^-$: Zeroes of angular observables as test of standard model,” arXiv:1412.2955 [hep-ph].
- [108] S. Jäger and J. Martin Camalich, “Reassessing the discovery potential of the $B \rightarrow K^* \ell^+ \ell^-$ decays in the large-recoil region: SM challenges and BSM opportunities,” arXiv:1412.3183 [hep-ph].
- [109] R. R. Horgan, Z. Liu, S. Meinel and M. Wingate, “Rare B decays using lattice QCD form factors,” arXiv:1501.00367 [hep-lat].
- [110] A. Crivellin, G. D’Ambrosio and J. Heeck, “Explaining $h \rightarrow \mu^\pm \tau^\mp$, $B \rightarrow K^* \mu^+ \mu^-$ and $B \rightarrow K \mu^+ \mu^- / B \rightarrow K e^+ e^-$ in a two-Higgs-doublet model with gauged $L_\mu - L_\tau$,” arXiv:1501.00993 [hep-ph].
- [111] S. Sahoo and R. Mohanta, “Scalar leptoquarks and the rare B meson decays,” arXiv:1501.05193 [hep-ph].
- [112] **LHCb** Collaboration, “Angular analysis of the $B^0 \rightarrow K^{*0} e^+ e^-$ decay in the low- q^2 region,” arXiv:1501.03038 [hep-ex].